Atmos. Chem. Phys. Discuss., 11, 16801–16859, 2011
www.atmos-chem-phys-discuss.net/11/16801/2011/
doi:10.5194/acpd-11-16801-2011

Atmospheric Chemistry and Physics Discussions

Future impact of non-land based traffic emissions on atmospheric ozone and OH – an optimistic scenario and a possible mitigation strategy

Ø. Hodnebrog[1], T. K. Berntsen[1], O. Dessens[2], M. Gauss[1,3], V. Grewe[4], I. S. A. Isaksen[1], B. Koffi[5], G. Myhre[6], D. Olivié[7], M. J. Prather[8], J. A. Pyle[2], F. Stordal[1], S. Szopa[5], Q. Tang[8], P. van Velthoven[9], J. E. Williams[9], and K. Ødemark[1]

[1]Department of Geosciences, University of Oslo, Norway
[2]Centre for Atmospheric Science, Department of Chemistry, Cambridge, UK
[3]Norwegian Meteorological Institute, Oslo, Norway
[4]Deutsches Zentrum für Luft- und Raumfahrt, Institut für Physik der Atmosphäre, Oberpfaffenhofen, Germany
[5]Laboratoire des Sciences du Climat et de l'Environment (LSCE-IPSL), Gif-sur-Yvette, France

[6] Center for International Climate and Environmental Research-Oslo (CICERO), Oslo, Norway
[7] Centre National de Recherches Météorologiques GAME/CNRM (Météo-France, CNRS), Toulouse, France
[8] Department of Earth System Science, University of California, Irvine, USA
[9] Royal Netherlands Meteorological Institute, KNMI, De Bilt, The Netherlands

Received: 20 April 2011 – Accepted: 1 June 2011 – Published: 16 June 2011

Correspondence to: Ø. Hodnebrog (oivind.hodnebrog@geo.uio.no)

Published by Copernicus Publications on behalf of the European Geosciences Union.

ACPD
11, 16801–16859, 2011

Abstract

The impact of future emissions from aviation and shipping on the atmospheric chemical composition has been estimated using an ensemble of six different atmospheric chemistry models. This study considers an optimistic emission scenario (B1) taking into account e.g. rapid introduction of clean and resource-efficient technologies, and a mitigation option for the aircraft sector (B1 ACARE), assuming further technological improvements. Results from sensitivity simulations, where emissions from each of the transport sectors were reduced by 5 %, show that emissions from both aircraft and shipping will have a larger impact on atmospheric ozone and OH in near future (2025; B1) and for longer time horizons (2050; B1) compared to recent time (2000). However, the ozone and OH impact from aircraft can be reduced substantially in 2050 if the technological improvements considered in the B1 ACARE will be achieved.

Shipping emissions have the largest impact in the marine boundary layer and their ozone contribution may exceed 4 ppb (scaled to 100 %) over the North Atlantic Ocean in the future (2050; B1) during northern summer (July). In the zonal mean, ship-induced ozone relative to the background levels may exceed 12 % near the surface. Corresponding numbers for OH are 6.0×10^5 molecules cm^{-3} and 30 %, respectively. This large impact on OH from shipping leads to a relative methane lifetime reduction of 3.92(±0.48) % on the global average in 2050 B1 (ensemble mean CH_4 lifetime is 8.0(±1.0) yr), compared to 3.68(±0.47) % in 2000.

Aircraft emissions have about 4 times higher ozone enhancement efficiency (ozone molecules enhanced relative to NO_x molecules emitted) than shipping emissions, and the maximum impact is found in the UTLS region. Zonal mean aircraft-induced ozone could reach up to 5 ppb at northern mid- and high latitudes during future summer (July 2050; B1), while the relative impact peaks during northern winter (January) with a contribution of 4.2 %. Although the aviation-induced impact on OH is lower than for shipping, it still causes a reduction in the relative methane lifetime of 1.68(±0.38) % in 2050 B1. However, for B1 ACARE the perturbation is reduced to 1.17(±0.28) %, which is lower than the year 2000 estimate of 1.30(±0.30) %.

ACPD

11, 16801–16859, 2011

Based on the fully scaled perturbations we calculate net radiative forcings from the six models taking into account ozone, methane (including stratospheric water vapour), and methane-induced ozone changes. For the B1 scenario, shipping leads to a net cooling with radiative forcings of $-28.0(\pm5.1)$ and $-30.8(\pm4.8)\,\mathrm{mW\,m^{-2}}$ in 2025 and 2050, respectively, due to the large impact on OH and thereby methane lifetime reductions. Corresponding values for the aviation sector shows a net warming effect with $3.8(\pm6.1)$ and $1.9(\pm6.3)\,\mathrm{mW\,m^{-2}}$, respectively, but with a small net cooling of $-0.6(\pm4.6)\,\mathrm{mW\,m^{-2}}$ for B1 ACARE in 2050.

1 Introduction

Increasing population and economic turnover will lead to increasing transport demand notably for aviation (AIR) and maritime shipping (SHIP). This will outpace technological improvements and lead to increasing emissions of various air pollutants, affecting air quality and climate through a complex system of chemical reactions and aerosol interactions. From a climate perspective, the present (2000) impact on radiative forcing (RF) is positive for AIR and negative for SHIP (Fuglestvedt et al., 2008; Balkanski et al., 2010), mostly due to formation of contrail cirrus in the first and sulphate in the latter. However, substantial contributions also stem from the emissions of nitrogen oxides (NO_x), carbon monoxide (CO) and non-methane hydrocarbons (NMHCs). These relatively short-lived gases change the oxidative state of the atmosphere and tend to give a positive radiative forcing through the increase in ozone (e.g., Ramanathan and Dickinson, 1979; Berntsen et al., 1997), while enhanced OH levels are known to reduce the lifetime of methane (CH_4) and thereby cause negative RF (e.g., Crutzen, 1987; Shindell et al., 2005). Among the various transport sectors, previous studies have shown that the warming effect is most efficient (relative to the number of NO_x molecules emitted) for AIR (e.g., Fuglestvedt et al., 2008) because changes in ozone have their largest impact on climate when they occur in the UTLS (upper troposphere/lower stratosphere) region, due to the low temperatures found near the tropopause (Wang and Sze, 1980;

ACPD
11, 16801–16859, 2011

Lacis et al., 1990; Hansen et al., 1997). On the other hand, the cooling effect caused by changes in methane lifetimes dominates the SHIP impact (e.g., Myhre et al., 2011) because of the large amounts of NO_x emitted into the clean maritime boundary layer. Due to the different effects on the atmospheric composition, it is important to study the AIR and SHIP sectors individually, especially when it comes to initiating mitigation measures. Another important aspect regarding non-land based traffic emissions, as opposed to land based traffic emissions, is the fact that the background conditions are usually relatively clean and this is known to increase the enhancement efficiencies of ozone and OH (e.g., Hoor et al., 2009).

IPCC (1999) published an assessment of the impact of aviation on climate, which was later updated by Sausen et al. (2005), and recently by Lee et al. (2009). Several other studies have also investigated how aircraft NO_x emissions alter the chemical composition of the atmosphere (e.g., Hidalgo and Crutzen, 1977; Johnson et al., 1992; Brasseur et al., 1996; Schumann, 1997; Grewe et al., 1999; Schumann et al., 2000; Kraabøl et al., 2002; Stevenson et al., 2004; Gauss et al., 2006; Grewe et al., 2007; Søvde et al., 2007). The studies dealing with impact from future subsonic aircraft NO_x emissions project an increase in aircraft-induced ozone in 2050 compared to the present day atmosphere, but the effect depends on the emission scenario used. Søvde et al. (2007) estimated a maximum zonal mean aircraft-induced ozone increase of about 10 ppbv in the UTLS region for 2050 (annual mean) (aircraft NO_x emissions of 2.18 $TgN\,yr^{-1}$). In another study, Grewe et al. (1999) calculated 7 to 10 % increased ozone mixing ratios due to aviation for the same year and region, but for two different emission scenarios (aircraft NO_x emissions of 2.15 and 3.42 $TgN\,yr^{-1}$, respectively).

Among the studies on impacts from ship emissions (e.g., Lawrence and Crutzen, 1999; Corbett and Koehler, 2003; Endresen et al., 2003; Eyring et al., 2005, 2007; Dalsøren and Isaksen, 2006; Endresen et al., 2007; Dalsøren et al., 2009, 2010), only one has made future projections with atmospheric chemistry models (Eyring et al., 2007). They project maximum near-surface ozone contributions from shipping of 5–6 ppbv (annual mean) in the North Atlantic for the year 2000, increasing to 8 ppbv in one

ACPD
11, 16801–16859, 2011

of the 2030 scenarios (ship NO_x emissions of 3.10 and 5.95 TgN yr^{-1}, respectively). In a second scenario ship emissions stabilized at 2000 levels, but the ozone impact decreased slightly due to higher background NO_x levels.

The present study is performed within the EU project QUANTIFY (Quantifying the Climate Impact of Global and European Transport Systems), which was the first attempt of investigating the global scale impact on the atmospheric composition due to emissions from each of the transport sectors. Fuglestvedt et al. (2008) investigated the climate forcing from the transport sectors for year 2000, and later Skeie et al. (2009) estimated transport-induced RF for future scenarios. A multi-model study of the year 2000 impact of transport emissions on the atmospheric chemical composition was performed by Hoor et al. (2009) using the preliminary QUANTIFY emissions. They found a maximum ozone increase from aircraft of 3.69 ppbv in the upper troposphere between 30–60° N, and they also found that shipping emissions contributed the most to ozone perturbations in the lower troposphere with around 50 % of the total traffic induced perturbation. The RF results from Hoor et al. (2009) were recently updated by Myhre et al. (2011) who used the final version of the QUANTIFY emissions data to estimate the year 2000 impact. The future impacts of both the emissions and climate changes on transport-induced ozone have so far only been studied by Koffi et al. (2010), using the climate-chemistry model LMDz-INCA (also used in this study). Main results obtained in QUANTIFY are summarized in Lee et al. (2010) (aviation), Eyring et al. (2010) (shipping), and Uherek et al. (2010) (land transport).

In this study we have investigated how emissions from the non-land based traffic sectors (AIR and SHIP) impact atmospheric ozone, OH, and the resulting RF, if emissions from all sectors evolve according to the SRES (Special Report on Emission Scenarios) optimistic B1 scenario (Nakicenovic et al., 2000). We have also studied the effect of utilizing additional technological improvements to the aircraft through the B1 ACARE mitigation option (Owen et al., 2010). The atmospheric chemistry models participating in this study have been run also with the SRES A1B emission scenario and with a policy failure emission scenario for road transport, A1B HIGH. Results from these

ACPD
11, 16801–16859, 2011

simulations are subject of followup studies. As the B1 scenario is considered to be far more optimistic than the A1B scenario (both for transport and non-transport emissions), due to assumptions of e.g. rapid introduction of clean and resource-efficient technologies in the first, the combined results represent possible low or high developments, respectively, of the transport-induced impact on the atmospheric chemical composition, taking into account uncertainties related to the evolution of e.g. economy and technology. More specifically, the B1 scenario is characterized by environmental concerns leading to improved NO_x technology and a relatively smooth transition to alternative energy systems, but without assumptions of climate policies (in accordance with the SRES terms of reference) (Nakicenovic et al., 2000). The fuel efficiency improvements in B1 ACARE probably requires the technology to be driven by concerns over climate change and is thus considered a mitigation scenario (Owen et al., 2010). In the following we describe the simulation setup and the emission scenarios (Sect. 2), before giving a short presentation of each of the models in the ensemble (Sect. 3). The impacts on ozone and OH are dealt with in Sects. 4 and 5, respectively, while global radiative forcing calculations are presented in Sect. 6. Finally, our conclusions are given in Sect. 7.

2 Emissions and simulation setup

Traffic emissions of the ozone precursors NO_x, CO and NMHC have been developed for year 2000 and for future scenarios through QUANTIFY (data can be downloaded from http://www.ip-quantify.eu). Anthropogenic emissions from non-traffic sources were taken from the EDGAR32FT2000 inventory (Olivier et al., 2005; van Aardenne et al., 2005) for year 2000, while the future non-traffic emissions evolve according to the IPCC (Intergovernmental Panel on Climate Change) SRES (Nakicenovic et al., 2000) B1 scenario. Table 1 lists the global annual emissions used in this study, and Fig. 1 shows the time development of NO_x emissions from different transport sectors and for several scenarios. Although the future increase in the global NO_x emissions from

ACPD
11, 16801–16859, 2011

AIR and SHIP is relatively small for the B1 scenario, important changes in the regional distribution of emissions can be seen for these transport sectors (Figs. 2–3).

New aircraft emissions scenarios have been developed using the FAST model and are described in Owen et al. (2010). B1 ACARE is a mitigation scenario for aviation and contains additional emission reductions on top of the reductions that are assumed in the B1 scenario. B1 ACARE can be seen as a very optimistic, but feasible scenario due to concern over climate change. The traffic demand is the same in both scenarios, but excellent fuel efficiency and NO_x improvements are assumed in the mitigation scenario, in accordance with the targets set by the Advisory Council for Aeronautical Research in Europe (ACARE, 2002). Consequently, the B1 ACARE scenario has 4 and 24 % lower aircraft NO_x emissions than B1 in 2025 and 2050, respectively, and the emissions for 2050 are even lower than the year 2000 estimate. Figure 2 shows that the increase in Europe and Asia in 2025 is smaller for B1 ACARE compared to the B1 scenario, and the emission reductions over the US are stronger in the first scenario. When comparing 2050 with 2025, only a few flight routes have increased emissions in B1 ACARE, and major emission reductions can be seen in Europe, the US, and Japan. The dependency of aircraft NO_x emissions on different latitude intervals can be seen in Fig. 3.

Shipping emissions are based on Endresen et al. (2007) (year 2000) and Eide et al. (2007) (years 2025 and 2050), and are characterized by increased NO_x emissions in the future, even for the optimistic B1 scenario. Already in 2025 the shipping sector could have become the largest emitter of NO_x among the three transport sectors (Fig. 1). Most of the increase for the B1 scenario is distributed among the 12 new shipping routes (Fig. 2) that are predicted by Eide et al. (2007). It is worth noting the Northern Sea Route which has increasing emissions from 2000 to 2025, and then shows a slight decline from 2025 to 2050.

Emissions from road transport are based on Borken et al. (2007). Future emissions are documented in Uherek et al. (2010). While road traffic was the dominating source of NO_x emissions among the transport sectors in 2000, assumptions of stricter vehicle

ACPD
11, 16801–16859, 2011

emission standards and improvements in technology will lead to a substantial decrease of NO_x emissions in the future scenarios (Fig. 1), particularly for B1. Technology with low NO_x emissions is already available for the road sector, and is faster to implement than for aircraft and shipping as the lifetime of vehicles is shorter. Koffi et al. (2010) showed that the rapid decline in NO_x emissions from road transport will lead to a drastic decrease in the ozone impact of road emissions in 2050. For this reason the impact of road traffic on ozone and OH has not been dealt with in this study, but model results from a policy failure scenario (A1B HIGH) for the road transport sector are subject of a followup study.

Additional emissions used in this study include biogenic emissions of isoprene and NO from soils (Jöckel et al., 2006), lightning NO_x emissions specified at 5 TgN yr^{-1} (Schumann and Huntrieser, 2007), and biomass burning emissions based on monthly mean Global Fire Emissions Database (GFED) estimates for 2000 (van der Werf et al., 2006) with multi-year (1997–2002) averaged activity data using emission factors from Andreae and Merlet (2001). Regarding methane, all models used prescribed surface boundary conditions for 2000, and most models updated the surface mixing ratios with values from IPCC (2001) for the future simulations.

The global models included in the ensemble have been run with year 2000 emissions and with the future emission scenarios B1 and B1 ACARE for the years 2025 and 2050. In all simulations, the meteorological data is from year 2003, while 2002 data was used to spin-up the models. For the year 2000 and for the future B1 simulations, a reference run (BASE) and perturbation runs, one for aircraft (AIR) and one for ship (SHIP), have been performed by each model for each year, while for B1 ACARE, only perturbed aircraft simulations have been performed in addition to new reference runs. In the perturbation simulations, a 5 % emission reduction has been applied to the respective traffic sector. The reasons not to switch off the emissions in the various transport sectors completely are both to reduce non-linearities in chemistry, and because the unscaled response of the chemical system is expected to be closer to the effect of realistic emission changes than a total removal of the emissions (Hoor et al.,

ACPD
11, 16801–16859, 2011

2009). The 5 % reduction approach was used to derive the sensitivity of the atmospheric chemical composition, e.g. ozone concentration, to an emission category with an appropriate accuracy (Hoor et al., 2009). The effect of, e.g. road traffic emissions is obtained by multiplying this sensitivity, e.g. change in ozone concentration per kg emission from road traffic, with the total road traffic emissions. When comparing results from this study with other studies, it is important to note that the 5 % perturbation approach is very different from removing an emission source by 100 %. Non-linearities in chemistry can lead to large differences between the two approaches as described in Hoor et al. (2009) and Koffi et al. (2010). For further discussions on the small perturbation approach, the reader is referred to Grewe et al. (2010). In order to simplify the comparison with Hoor et al. (2009) and Myhre et al. (2011), the ozone and OH results (Sects. 4 and 5.1) are shown unscaled, while calculations of methane lifetime changes and radiative forcings (Sects. 5.2 and 6) have been scaled to 100 %.

3 Model descriptions

An ensemble of six models has been applied in order to estimate the future impact of non-land based traffic emissions on atmospheric ozone and OH, when considering optimistic scenarios. For the results presented in Sects. 4–6, equally weighted average values of the six models are shown along with the standard deviations, representing the spread in the model results (selected individual model results are shown in Appendix A). Five global Chemistry Transport Models (CTMs) were driven by meteorological data from the European Centre for Medium-Range Weather Forecasts (ECMWF), and one Climate Chemistry Model (CCM) was nudged towards the ECMWF data. The models have been evaluated by Schnadt et al. (2010). General model properties are listed in Table 2, and short descriptions are given below.

ACPD
11, 16801–16859, 2011

3.1 TM4

TM4 is a 3-D global chemistry transport model with a horizontal resolution of $3^\circ \times 2^\circ$ and 34 vertical layers up to 0.1 hPa. It is driven by ECMWF meteorological operational data which is updated every 6 h. The version used here has been comprehensively described in Williams et al. (2010). The chemical scheme is the modified CBN4 mechanism decribed by Houweling et al. (1998), supplemented with sulphur chemistry and with the chemical reaction data being updated by Williams and van Noije (2008). The advection scheme is the slopes method developed by Russell and Lerner (1981), while convection is based on the Tiedkte mass flux scheme (Tiedtke, 1989). A one year spin-up period for the year 2002 was used prior to the simulation year used for this study.

3.2 p-TOMCAT

The global offline chemistry transport model p-TOMCAT is an updated version (see O'Connor et al., 2005) of a model previously used for a range of tropospheric chemistry studies (Law et al., 1998, 2000; Savage et al., 2004). The model is used here with a horizontal resolution of $5.6^\circ \times 5.6^\circ$ (T21) and extends from the surface to 10 hPa in 31 vertical levels. The offline meteorological fields are from the operational analyses of the ECMWF model.

The chemical mechanism includes the reactions of methane, ethane and propane plus their oxidation products and of sulphur species. The model chemistry uses the atmospheric chemistry integration package ASAD (Carver et al., 1997) and is integrated with the IMPACT scheme of Carver and Stott (2000). The chemical rate coefficients used by p-TOMCAT are taken from the IUPAC summary of March 2005. The Prather (1986) scheme is used for advection while convective transport is based on the mass flux parameterization of Tiedtke (1989).

ACPD
11, 16801–16859, 2011

3.3 OsloCTM2

OsloCTM2 is a 3-D chemistry transport model driven by ECMWF meteorological data (Gauss et al., 2003; Søvde et al., 2008). The version used for this study includes both tropospheric and stratospheric chemistry, and it extends from the surface to 0.1 hPa in 60 vertical layers. A horizontal resolution of Gaussian T42 (2.8° × 2.8°) was used. The model was run with the various QUANTIFY emission scenarios for 30 months, the first 18 of which used as spin-up and the last 12 for analysis. Advection in OsloCTM2 is done using the second order moment scheme (Prather, 1986), while convection is based on the Tiedtke mass flux scheme (Tiedtke, 1989). The Quasi Steady-State Approximation (Hesstvedt et al., 1978) is used for the numerical solution in the chemistry scheme, and photodissociation is done on-line following Wild et al. (2000).

3.4 LMDz-INCA

The LMDz-INCA model consists of the LMDz General Circulation Model (Le Treut et al., 1998), coupled on line with the chemistry and aerosol model INCA (Folberth et al., 2006). The version 4.0 of the LMDz model has 19 hybrid levels on the vertical from the ground to 3 hPa and a horizontal resolution of 2.5° in latitude and 3.75° in longitude (96 × 72 grid cells). The large-scale advection of tracers is performed using the finite volume transport scheme of Van Leer (1977), as described in Hourdin and Armengaud (1999). The turbulent mixing in the planetary boundary layer is based on a second-order closure model. The INCA model considers the surface and 3-D emissions, calculates dry deposition and wet scavenging rates, and integrates in time the concentration of atmospheric species with a time step of 30 min. The CH_4-NO_x-CO-O_3 photochemistry, as well as the oxidation pathways of non-methane hydrocarbons and non-methane volatile organic compounds are taken into account.

ACPD
11, 16801–16859, 2011

3.5 UCI CTM

In this study, the University of California, Irvine (UCI) chemistry transport model (CTM) is driven by year 2002 and 2003 meteorological data from the ECMWF Integrated Forecast System (IFS) cycle 29r2 developed by U. Oslo (Kraabøl et al., 2002; Isaksen et al., 2005). The model extends from the surface to 2 hPa with 40 vertical layers and is run at T42 horizontal resolution with the QUANTIFY present and future emission datasets for 24 months (methane is fixed at tropospheric abundance of 1760 ppb). The first 12-month run is used as spin-up and the results from the last 12 are analyzed here.

The UCI CTM contains separate tropospheric and stratospheric chemistry. The tropospheric chemistry is simulated by the ASAD (A Self-contained Atmospheric chemistry coDe) software package (Carver et al., 1997) with UCI updates (Tang and Prather, 2010), which include the chemical kinetics and photochemical coefficients from the JPL publication 06–2 (Sander et al., 2006), and quasi steady-state initial guesses for radicals, and $O(^1D)$ included with O_3. The stratospheric chemistry uses the linearized ozone scheme (Linoz), which can include up to four independent species (e.g., O_3, N_2O, NO_y, CH_4), but in this case consists only ozone (Prather and Hsu, 2010). The tropopause, the boundary between the troposphere and the stratosphere, is determined by an artificial tracer (e90) (Prather et al., 2011; Tang et al., 2011). The advection and convection use the same schemes as OsloCTM2.

3.6 MOCAGE

MOCAGE is a 3-D-chemistry transport model driven by ECMWF analyses (Teyssèdre et al., 2007). It is used here with a horizontal resolution of $5.6^\circ \times 5.6^\circ$ (T21) and 60 levels up to 0.1 hPa, and contains both tropospheric and stratospheric chemistry. The large-scale transport of the tracers is done using a semi-Lagrangian transport scheme (Williamson and Rasch, 1989), while the convective transport is as described in Bechtold et al. (2001). The model was run for two years, and the second year was used for analysis.

ACPD
11, 16801–16859, 2011

4 Ozone

The 2050 B1 annual mean ozone column response to a 5 % perturbation in emissions is shown in Fig. 4 for the aircraft and shipping sectors. The ozone impact from AIR is zonally well mixed, and mostly confined to the Northern Hemisphere (NH) in accordance with the latitudinal distribution of emissions shown in Fig. 3. Scaling up the impacts following the approach of Grewe et al. (2010) results in a maximum ozone column response of 1.6 DU. The corresponding perturbation for SHIP is also 1.6 DU, but much less homogeneously distributed with maximum values occurring over the North Atlantic Ocean and at the coastal areas of South East Asia. These two areas were also identified as peaks in the 2030 model simulations performed by Eyring et al. (2007), who attributed the increased ship-induced tropospheric ozone column over the Indian Ocean to the higher tropopause and more effective vertical transport found there.

Figure 4 also shows the relative standard deviation which represents the spread in results between the different models (see Appendix A for individual model results). Only results for 2050 B1 are shown in Fig. 4, but the relative standard deviations for the other years and scenarios also have similar distributions. The robustness of the models is quite good for the aircraft perturbation case, with a relative standard deviation less than 20 % in most of the areas where the perturbation effect is strong. However, model differences in interhemispheric transport result in a larger relative standard deviation in the Southern Hemisphere (SH). The relative standard deviation for shipping demonstrates larger deviations between the models compared to the aircraft case, and is mainly in the range 30–40 %. One of the models (OsloCTM2) gives large impacts from shipping with a scaled maximum value of 2.5 DU, while another model (MOCAGE) has a corresponding value of only 0.9 DU. However, as model intercomparison is beyond the scope of this study, the reader is referred to e.g., Danilin et al. (1998) and Rogers et al. (2002) for thorough discussions of differences between CTMs.

ACPD
11, 16801–16859, 2011

4.1 Effects of aircraft emissions

Figure 5 shows the impact from aircraft emissions on ozone in the UTLS region for January and July. When focusing on the B1 scenario, the results indicate an increase in ozone impact from aircraft between 2000 and 2025, while the difference between 2025 and 2050 depends on the season and on the latitude. Because of the strong net decrease in NO_x emissions from aircraft at northern mid- and high latitudes from 2025 to 2050 (Fig. 3), the resulting ozone effect is a decrease in zonal mean values north of 30° N during summer (Fig. 5) when the photochemistry is more intense. This signal is to a large extent consistent between the models, but whether or not there is an ozone decrease in the NH during winter depends strongly on the model. In the SH, the ozone impact from aircraft emissions is likely to increase in 2025 and further to 2050, if emissions evolve according to the B1 scenario. The zonal mean local maximum of 0.066 ppbv (or 1.3 ppbv scaled to 100 %) at about 30° S in 2050 B1 (July) is caused by a combination of increased emissions in the tropics and transport across the hemispheres.

The local maximum can also be seen in Fig. 6, which shows the zonal mean ozone impact for 2050 B1 (see Fig. A1 for individual model results), together with the average vertical profile of the NH impact on ozone for each year and scenario. The results show that the maximum absolute impact in the UTLS region is larger in July compared to January, because of the variability in the length of the day between both months. However, the maximum ozone impact relative to the reference simulation (BASE) in 2050 B1 is larger in January with a peak value of 0.21 % (or 4.2 % scaled) located in the middle to upper troposphere at 20–30° N. For comparison, Grewe et al. (1999) calculated annual maximum relative ozone changes due to aircraft emissions of 7 % in a 2050 scenario, but the aircraft NO_x emissions used in their study were about twice as large as the 2050 B1 emissions that are used here (2.15 $TgN\,yr^{-1}$ compared to 1.05 $TgN\,yr^{-1}$), and the surface NO_x emissions were 60 % larger (69.7 $TgN\,yr^{-1}$ compared to 43.8 $TgN\,yr^{-1}$). The difference in year of meteorology used will also have an

ACPD
11, 16801–16859, 2011

influence on the comparison. Also worth noting is the fact that ozone perturbations in the lower troposphere are weaker during summer than in winter, presumably because the surface deposition to plants is faster and the photochemical lifetime of ozone is shorter (because increased water vapour gives more HO_X and thereby ozone loss) at lower altitudes during summer.

If emissions evolve according to the B1 ACARE mitigation option rather than the B1 scenario, Figs. 5 and 6 show that ozone will only be reduced by a small amount in 2025, while in 2050 the mitigation option will have a substantial effect on reducing ozone levels. A direct comparison between B1 and B1 ACARE yields mean ozone differences poleward of 30° N in the UTLS of 0.18–0.30 ppbv and 0.94–1.40 ppbv during summers of 2025 and 2050, respectively (Fig. 5). Notably in the NH, the average ozone perturbation from aircraft in 2050 for B1 ACARE is reduced to considerably lower values than the estimated impact in year 2000 for altitudes below 200 hPa (Fig. 6). The fact that the mitigation option only has a minor effect in 2025 could be associated with the long lifetime of aircraft.

Hoor et al. (2009) found that the change in ozone burden per NO_x-emission was highest for aircraft when comparing with the road and ship transport sectors. In Table 3 we have presented the ozone enhancement efficiency in order to investigate how the sensitivity changes with different years and scenarios. Previous studies (e.g., Grooss et al., 1998; Grewe et al., 1999) have found that the non-linearity in the ozone production normally leads to a smaller positive ozone perturbation per aircraft emitted NO_x-molecule when the emissions are higher. This is also the case when we compare the ozone change per aircraft NO_x-emission in 2000 with 2025 (Table 3), when the emissions are expected to increase. However, when looking at the 2050 B1 scenario, all models show a higher ozone enhancement efficiency compared to year 2000, although the aircraft NO_x emissions also are higher. This unexpected effect could be explained by higher background methane levels which would make the ozone production more effective, and by the change in the location of the emissions. In 2050, the aircraft NO_x emissions are shifted further south compared to year 2025 (Fig. 3), and will then take

ACPD
11, 16801–16859, 2011

place in more pristine regions where the background NO_x levels are lower. Additionally, Hoor et al. (2009) emphasized the role of road traffic for the chemical state of the UTLS, and as NO_x emissions from this transport sector are assumed to decrease rapidly in the future, the NO_x background levels at cruise altitude are affected. Not surprisingly, the highest ozone enhancement efficiency is found in 2050 B1 ACARE, which is the scenario with the lowest aircraft emissions. For this case, the models estimate that the ozone abundance increases by 2.31 molecules for every NO_x molecule emitted from aircraft.

4.2 Effects of ship emissions

Figures 7 and 8 show the effects of shipping emissions on atmospheric ozone in January and July for different years and scenarios (see Fig. A2 for individual model results). Even if emissions evolve according to the optimistic B1 scenario, model results show that the shipping sector will increase its effect on ozone in the future. Focusing on the estimated ozone impact in the lower troposphere in 2050 B1 (Fig. 7), the largest effect from shipping can be found in the North Atlantic Ocean with ozone values of about 0.2 ppbv (or 4 ppbv scaled) during summer when the photochemical activity reaches a maximum. Notably, the impact in the Arctic region is expected to increase in the future due to the expected introduction of new ship tracks associated with melting of the polar ice cap. This area is especially sensitive to emission perturbations because of the low background NO_x levels which lead to higher ozone enhancement efficiencies. Consequently, the maximum relative effects in July are found in this region, showing zonal mean impacts exceeding 0.6 % (or 12 % scaled) near the surface (Fig. 8).

Interestingly, Fig. 7 shows that the ozone impact from shipping at northern mid- and high latitudes will increase from 2025 to 2050, especially during winter, although the emissions in these regions are expected to decrease (Fig. 3). Except for transport from lower latitudes, where the emissions increase, this feature can be explained by lower ambient levels of NO_x which act to increase the change in ozone burden per NO_x emitted from ships. The increase in ozone enhancement efficiency can also be seen

ACPD
11, 16801–16859, 2011

in Table 3, where global annual average values are given. In the future B1 scenario, large reductions in anthropogenic non-traffic and road emissions of NO_x are assumed over the Eastern US and Europe. This significantly increases the ozone enhancement efficiency from shipping, as transport from these polluted continental areas normally leads to higher levels of NO_x over the Atlantic Ocean and the North Sea.

5 OH

5.1 Global OH

Changes in the concentration and distribution of the hydroxyl radical (OH) are important for air pollution and the self-cleaning capacity of the atmosphere (Lelieveld et al., 2002) as OH is the main oxidant in the troposphere. Validation of modelled OH is difficult, however, particularly because of its short lifetime (less than one second) which makes it almost impossible to measure directly. In a recent study by Montzka et al. (2011), indirect measurements of the interannual variability of global OH are consistent with past model studies (Dentener et al., 2003; Dalsøren and Isaksen, 2006; Lelieveld et al., 2006; Duncan and Logan, 2008), and this suggest that larger confidence should be given to models than previously assumed (Isaksen and Dalsøren, 2011).

The impact of aircraft and shipping emissions on tropospheric OH is shown in Figs. 9 and 10 for July, when the effect is largest due to enhanced photochemistry in the NH. For aircraft emissions, there is an indication of a future increase in the impact on tropospheric OH. Figure 9 shows that enhanced OH levels in the UTLS are expected at all latitudes in 2025, with an exception near the Arctic region where increased aircraft emissions seem to cause a slight decrease in OH levels. However, when comparing the impacts between 2025 and 2050, the OH response depends strongly on both scenario and latitude. In 2050, a decrease is seen between approximately 30° N–60° N, associated with a strong decrease in aircraft NO_x emissions (Fig. 3), while a zonal mean increase is expected elsewhere, in particular near the equator where aircraft

ACPD
11, 16801–16859, 2011

NO_x emissions are assumed to increase. In 2025 B1, the zonal mean average in the UTLS region for July peaks at 40° N with a value of 8.6×10^3 molecules cm^{-3} (unscaled). When averaging the aircraft-induced OH vertical profile over the entire NH, 2025 B1 and 2050 B1 both shows a maximum of 5.4×10^3 molecules cm^{-3} (unscaled) near 250 hPa (Fig. 10).

The largest effects from aircraft emissions during northern summer in the future (July 2050; B1) can be found east and southeast of Asia, but also with significant impacts close to the North Atlantic flight corridor (Fig. 9). The zonal mean OH impact peaks above 300 hPa, and this is also the region of maximum relative impact with a value of 0.6 % (or 12 % scaled) (Fig. 10). In the SH, the absolute values are lower, but due to low background levels the relative impact is fairly high with a value of almost 0.5 % (or 10 % scaled).

As was the case with ozone, the technological improvements that are assumed in the B1 ACARE mitigation scenario have significant effects on OH. If the ACARE targets will be met in 2050, the northern summer OH levels in the UTLS region could be reduced by up to 5.7×10^4 molecules cm^{-3} (Fig. 9). The reductions are substantial also in the NH as a whole, showing average differences between B1 and B1 ACARE of 3.9×10^4 molecules cm^{-3} near 250 hPa (Fig. 10), and with significant effects also in the middle troposphere. In the near future (2025), the gain of fulfilling the ACARE targets is much lower, but still the maximum difference between B1 and B1 ACARE is 7.6×10^3 molecules cm^{-3}.

Hoor et al. (2009) emphasized the large impact of ship emissions on the boundary layer OH levels, and concluded that the effect of ship emissions is more important for the global OH budget than road and aircraft emissions. Figure 9 shows that the impact from ship emissions on OH in the boundary layer is expected to increase in the future if emissions evolve according to the B1 scenario. Between 2025 and 2050, OH will continue to increase at all latitudes except north of 60° N where a small reduction in ship NO_x emissions is expected.

ACPD
11, 16801–16859, 2011

Focusing on northern summer in the future (July 2050; B1), the largest impact from ship emissions can be found in the North Atlantic Ocean with maximum values reaching 3.0×10^4 molecules cm^{-3} (unscaled) (Fig. 9). As discussed in Sect. 4.2, ozone production in this area is largely sensitive to an increase in NO_x emissions, and because of high humidity and strong incoming solar radiation, additional OH is produced when $O(^1D)$ reacts with H_2O. Additionally, the background levels of CO and NMHCs, which act to deplete OH, are relatively low in these pristine regions. In the zonal mean, maximum absolute values are found near the surface at 45° N (Fig. 10), while the relative impact reaches a maximum of about 1.5 % (or 30 % scaled) near 75° N. The reason is the low background values of OH, as shipping is a dominant source of air pollutants at these high latitudes, and because the production of additional OH caused by ship emissions is more effective in the summer month of July.

5.2 Methane lifetime

Emissions from the aircraft and shipping sectors greatly affect the OH concentration, and this leads to changes in the methane lifetime. Methane lifetimes due to reaction with OH have been calculated for each model and for each year and scenario, using the same method as described in Hoor et al. (2009). Monthly mean 3-D-fields of methane and OH were used, and the resulting lifetime changes were then scaled from a 5 % perturbation in emissions to a 100 % perturbation (to get a stronger signal in the RF calculations) by multiplying with a factor of 20 (Grewe et al., 2010). The resulting model mean and standard deviation of the methane lifetime changes are given in Table 4 (see Tables A1 and A2 for individual model results), while the model mean of the methane lifetime is 8.0(±1.0) yr in the 2050 B1 BASE simulation and 8.3(±1.0) yr in the 2000 BASE simulation. The rather low relative standard deviation of 12 % is similar for the BASE simulations of the other scenarios, and indicates that the ensemble mean of the models is relatively robust when calculating methane lifetimes.

As discussed in Sect. 5.1, SHIP exhibits the largest impact on OH levels and consequently the largest impact on methane lifetime. The model ensemble predicts that

ACPD
11, 16801–16859, 2011

the shipping sector contributed to a methane lifetime reduction of 3.68 % in year 2000, and that this number will increase to 3.92 % in 2050, if emissions evolve according to the B1 scenario (Table 4). Eyring et al. (2007) calculated methane lifetime changes from shipping in 2030, and their estimates range from 1.14 % to 1.81 % for a low and high emission scenario, respectively. Their result is much lower than both 2025 B1 and 2050 B1 from this study, and that was also the case for the year 2000 results discussed in Hoor et al. (2009). According to Hoor et al. (2009), part of the differences could be attributed to the very different distribution of ship emissions. The same reasoning applies here as the future ship emissions in Eyring et al. (2007) are more concentrated along the major shipping routes in contrast to the QUANTIFY future ship emissions, which are spread out over larger areas.

The methane lifetime changes for SHIP do not follow the trend in ship NO_x emissions, which increased a lot more between 2000 and 2025 B1 than between 2025 B1 and 2050 B1 (Fig. 1). The reason could be the assumption of large reductions in land based NO_x emissions, particularly from road traffic, in Europe and the US between 2025 B1 and 2050 B1. This effect may exceed the impact of increased ship emissions, as a decrease in background NO_x levels leads to a more efficient OH production from shipping.

The future methane lifetime changes for AIR are to a certain degree in accordance with the evolution of the aircraft B1 emission scenarios; an increased impact in 2025 followed by stabilization in 2050 (Table 4). The model ensemble predicts a much lower impact of aircraft on methane lifetimes for the B1 ACARE scenario, especially in 2050 when the relative methane lifetime change is lower than the year 2000 value.

6 Radiative forcings

Radiative forcings have been calculated using the same method as in Myhre et al. (2011). The Oslo radiative transfer model (Myhre et al., 2000) was used to calculate ozone radiative forcings based on monthly mean ozone fields from each model

ACPD
11, 16801–16859, 2011

simulation. In order to obtain a robust signal the fully scaled perturbations have been used in the RF calculations, i.e. the ozone change resulting from the 5 % perturbation has been multiplied by 20 (Hoor et al., 2009; Grewe et al., 2010). According to Myhre et al. (2011), the non-linearities arising from the perturbation magnitude are of little importance compared to the inter-model differences in the RF.

Figure 11 shows the yearly averaged ozone RF for the 2050 B1 scenario as means of all models and with absolute standard deviations. The aircraft sector has a larger impact than ship emissions in the NH and the changes in RF are relatively homogeneous throughout different latitude zones. The impacts are large throughout the NH and have maximum values reaching 76 m W m^{-2} near 30° N. In the SH the ozone RF from aircraft is low, except in the region 0–30° S. This latitude band also shows a large spread of the models with standard deviations up to 21 m W m^{-2}, indicating possible model uncertainties related to convection and transport between the hemispheres. For SHIP, the ozone RF is stronger in the SH compared to AIR, but the RF in the NH is much weaker. Maximum impact from SHIP takes place between 30° N and 30° S, and peaks at 50 m W m^{-2}.

Global average ozone RF for all scenarios is given in Table 5 (see Tables A3 and A4 for individual model results). For the B1 scenario there is a small increase in the ozone RF from AIR between 2025 and 2050, although the NO_x emissions from aircraft are assumed to decrease slightly during this time span. As explained in Sect. 4.1, this is probably caused by the latitudinal shift in the location of the aircraft emissions leading to higher ozone enhancement efficiencies in 2050. For comparison, Myhre et al. (2011) calculated a five model average of 17 m W m^{-2} for AIR in year 2000. The increase to 25.7 m W m^{-2} for 2025 B1 (Table 5) is consistent with the aircraft NO_x emissions, which also are assumed to increase (Fig. 1). For the 2050 B1 scenario, Skeie et al. (2009) estimated ozone RF from AIR to be 38 m W m^{-2} using a simple climate model. The relatively large difference to our study can be partly explained by a lower normalized radiative forcing in this study (36.3 compared to 42.9 m W m^{-2} DU^{-1}), and partly by lower ozone enhancement efficiencies (2.16 compared to 2.69 ozone molecules enhanced

ACPD
11, 16801–16859, 2011

per NO_x molecule emitted from AIR). In Lee et al. (2009), a scaling approach was used to estimate the aviation RF of ozone in 2050 to be in the range 59.4–109.8 m W m^{-2}, depending on the scenario. Their estimates are much higher than in this study, but this is expected because even their lowest emission scenario (SRES B2 with technology 2, see IPCC, 1999) had larger aircraft NO_x emissions than the 2050 B1 scenario used here. The effect of the B1 ACARE mitigation strategy is evident already in 2025, with a 1.6 m W m^{-2} lower ozone RF than in the B1 scenario (Table 5). However, in 2050 the corresponding number has increased to 7.3 m W m^{-2}, showing the large potential of technological improvements in the aircraft sector.

The ozone RF from SHIP is calculated to increase between 2025 and 2050, this time due to a combination of the slight increase in ozone precursor emissions for this transport sector, and the stronger ozone enhancement efficiency in 2050 (see Sect. 4.2). Despite the assumed increase in ship emissions between 2000 and 2025 B1, Myhre et al. (2011) has a larger estimate for 2000 (24 m W m^{-2}) than our results for 2025 B1. The reason is that the MOCAGE model is included in our study, and this model is at the lower end of the spectrum when calculating ozone RF from SHIP (not shown). Again, Eyring et al. (2007) calculated lower impacts than in this study, with ozone RF from shipping ranging from 7.9 to 13.6 m W m^{-2} in 2030. On the other hand, Skeie et al. (2009) estimated a larger impact from shipping with short-lived ozone RF at 36 m W m^{-2} for the 2050 B1 scenario, also this time due to lower ozone enhancement efficiencies in this study (0.535 compared to 0.859 ozone molecules enhanced per NO_x molecule emitted from SHIP).

Emissions of NO_x from aircraft and shipping sectors normally lead to an increase in OH concentrations, resulting in a reduction of methane lifetime. The forcing due to the changes in methane is given in the second column in Table 5, and has been calculated mainly using the method described by Berntsen et al. (2005). For each year and scenario, the changes in methane lifetime were multiplied by the estimated methane concentrations reported in IPCC (2001). Further, to account for the impact of methane changes on its own lifetime, a feedback factor of 1.4 was used (IPCC, 2001).

ACPD
11, 16801–16859, 2011

The linearized methane specific forcing of 0.35 m W m^{-2} ppbv^{-1} was then applied, assuming a background methane mixing ratio of 1909 ppb and 1881 ppb for 2025 B1 and 2050 B1, respectively. In Table 5, the CH_4 RF term includes the impact of methane changes on stratospheric water vapour (SWV), and the RF of SWV is assumed to be 0.15 times that of the methane RF (Myhre et al., 2007).

RF from changes in methane-induced ozone is calculated assuming that a 10 % increase in methane leads to a 0.64 DU increase in ozone (IPCC, 2001), and that this ozone has a specific forcing of 42 m W m^{-2} DU^{-1} (IPCC, 2001). As explained in Myhre et al. (2011), the chemical model calculations are one year simulations only, hence the methane concentration may not be in steady state with the change in OH during that year, but dependent on the time-history of the emissions. In order to correct for this transient response, factors have been applied based on the method described in Grewe and Stenke (2008). The factors for 2025 are 0.88, 0.91 and 0.94 for AIR B1, AIR B1ACARE and SHIP B1, respectively. Corresponding factors for 2050 are 1.00, 1.15 and 0.99. Note that the factor for 2050 B1 ACARE is larger than 1 because the aircraft emissions are assumed to decrease in the preceeding years for this scenario.

The sum of the three RF components in Table 5 shows a negative RF from SHIP, and this is consistent with what has been found in previous studies (Fuglestvedt et al., 2008; Skeie et al., 2009; Myhre et al., 2011). For AIR, however, the total RF is slightly positive in three out of four cases. Interestingly, a slightly negative RF is predicted for the 2050 B1 ACARE scenario. It is important to note that the net effect for AIR is the sum of a fairly large positive number (O_3 RF) and two smaller negative numbers (CH_4 plus induced O_3 RF), each associated with uncertainties. The subtle difference between these effects results in a small net value, and considering the uncertainties it is difficult to say for sure whether or not the net effect is positive or negative. However, the general tendency of an increasing importance of methane RF relative to the ozone RF for future air traffic emissions is consistent for both B1 scenarios. It reflects the decreasing rate of ozone RF increase, whereas the CH_4 RF decreases are effective with a time-lag associated with the methane lifetime. For the B1 scenario, a reduction of

ACPD
11, 16801–16859, 2011

1.9 m W m^{-2} is predicted between 2025 and 2050, and for B1 ACARE the reduction is 3.5 m W m^{-2}. Compared to Myhre et al. (2011), our estimates of total RF may seem low considering that the aircraft NO_x emissions are higher for the B1 scenario in 2025 and 2050 than they were in 2000. The reason is related to the factors used to correct for the time-history of the emissions, which has to be kept in mind when interpreting RF from methane plus induced ozone changes. The aircraft NO_x emissions increased rapidly prior to year 2000, while the increase levelled off towards 2025, and further turned to a reduction towards 2050 in the B1 and B1 ACARE scenarios. As a consequence, the cooling effect caused by changes in methane and methane-induced ozone RF may compensate the warming from short-term ozone RF (which is unaffected by the time-history of emissions), if emissions evolve according to the optimistic B1 or B1 ACARE scenarios.

7 Conclusions

Six atmospheric chemistry models have been applied in order to investigate how emissions from the non-land based traffic sectors (AIR and SHIP) impact the distributions of ozone and OH according to the B1 and B1 ACARE emission scenarios. Although the B1 scenario is considered optimistic, model results show that the impacts of both AIR and SHIP emissions on ozone and OH will increase in the future (2025 and 2050) compared to recent time (2000). We used the perturbation approach to calculate both, the contributions of the individual sectors to ozone and OH, and their changes over time, knowing that this methodology has principle limitations in the calculation of contributions (Grewe et al., 2010). The choice of −5 % emission perturbations guarantees a consistent calculation of the atmospheric sensitivity with respect to aircraft and ship emissions (Hoor et al., 2009). Our contribution calculation highlights the large impact of ship emissions on the chemistry in the lower troposphere, and indicates that ship-induced ozone could exceed 4 ppb over the North Atlantic Ocean during future summer (July 2050; B1). At the same time, aircraft emissions dominate in the UTLS region with a maximum zonal mean ozone impact that could reach 5 ppb polewards of 30° N.

ACPD
11, 16801–16859, 2011

Model simulations with the B1 ACARE mitigation scenario for aviation show modest reductions in ozone levels in 2025, while substantial reductions can be expected in 2050. Zonal means of the UTLS region at northern mid- and high latitudes show that B1 ACARE yields 0.9–1.4 ppb lower ozone values than the already optimistic B1 scenario during future summer (July 2050), and this is even lower than for recent time (2000). However, all of our future simulations predict an increase in aircraft-induced ozone in the SH compared to year 2000, and this is mainly a response to the assumed increase in aircraft NO_x emissions in this region. Additionally, the shift in emission location between 2025 and 2050, from the already polluted mid- and high northern latitudes to the more pristine regions in the south, leads to an increase in the ozone enhancement efficiency with an increase in the ozone concentration of 2.31 molecules per emitted aircraft NO_x molecule for the 2050 B1 ACARE scenario.

Emissions from SHIP have important effects on the OH concentrations, particularly in the marine boundary layer, and this impact will become increasingly important in the future. As a consequence, the models estimate a relative methane lifetime reduction of 3.9 % (scaled) due to SHIP in 2050 B1. The corresponding value for AIR is 1.7 %, but if the ACARE targets will be achieved, this number is reduced to 1.2 %.

The large impact of SHIP on OH is reflected in the radiative forcing calculations. When considering RF from changes in short-term ozone, methane (including stratospheric water vapour), and methane-induced ozone, our results suggest that SHIP will have a net cooling effect in 2025 and 2050 of $-28.0(\pm5.1)$ and $-30.8(\pm4.8)\,\mathrm{mW\,m^{-2}}$, respectively, for the B1 scenario. The uncertainties relative to net RF are larger for AIR, but positive RF from short-term ozone normally dominates. The resulting RF for AIR in the B1 scenario is $3.8(\pm6.1)$ and $1.9(\pm6.3)\,\mathrm{mW\,m^{-2}}$ in 2025 and 2050, respectively. Interestingly, a small cooling effect of $-0.6(\pm4.6)\,\mathrm{mW\,m^{-2}}$ is estimated for 2050 B1 ACARE, but it is important to note that the time-history of emissions has been taken into account, and this leads to a dominance of RF caused by changes in methane and methane-induced ozone, as the larger aviation emissions prior to 2050 have no impact on the 2050 short-term ozone RF (due to shorter lifetime of ozone compared

ACPD
11, 16801–16859, 2011

to methane). In order to obtain knowledge of the total impact from AIR and SHIP on future climate, the RF from CO_2, contrails (including contrail-cirrus) and aerosols must be considered in addition to the RF from ozone and methane presented here.

To summarize, emissions from the two transport sectors aviation and shipping will have an increased impact on atmospheric ozone and OH in the future, even if emissions evolve according to the optimistic B1 scenario. However, the aviation impact through ozone formation can be reduced significantly by initiating the ACARE mitigation option, which is purely based on technological improvements. The long operating time of aircraft suggests that mitigation measures for this traffic sector should be considered at an early stage.

Appendix A

Results from individual models

Individual model results are shown for the 2050 B1 scenario as zonal mean ozone perturbations for AIR and SHIP in Figs. A1 and A2, respectively. Relative changes in methane lifetimes are listed in Tables A1 and A2, and RF calculations are given in Tables A3 and A4.

Acknowledgements. This work was funded by the European Union's Sixth Framework Programme (FP6/2002–2006) through the QUANTIFY Integrated Project under contract no. 003893 (GOCE), and through the Network of Excellence ECATS (Project no. ANE4-CT-2005-012284). Emission data sets were provided by the QUANTIFY partners MMU (aircraft), DNV (shipping), DLR (road traffic) and JRC (other anthropogenic emissions). The authors would like to thank Jens Borken-Kleefeld (IIASA) and Magnus S. Eide (DNV) for their helpful comments on the manuscript.

ACPD
11, 16801–16859, 2011

References

ACARE: Strategic Research Agenda, Advisory Council for Aeronautics Research in Europe, Brussels, 2002.

Andreae, M. O. and Merlet, P.: Emission of trace gases and aerosols from biomass burning, Global Biogeochem. Cy., 15, 955–966, 2001.

Balkanski, Y., Myhre, G., Gauss, M., Rädel, G., Highwood, E. J., and Shine, K. P.: Direct radiative effect of aerosols emitted by transport: from road, shipping and aviation, Atmos. Chem. Phys., 10, 4477–4489, doi:10.5194/acp-10-4477-2010, 2010.

Bechtold, P., Bazile, E., Guichard, F., Mascart, P., and Richard, E.: A mass-flux convection scheme for regional and global models, Q. J. Roy. Meteor. Soc., 127, 869–886, 2001.

Berntsen, T. K., Isaksen, I. S. A., Myhre, G., Fuglestvedt, J. S., Stordal, F., Larsen, T. A., Freckleton, R. S., and Shine, K. P.: Effects of anthropogenic emissions on tropospheric ozone and its radiative forcing, J. Geophys. Res.-Atmos., 102, 28101–28126, 1997.

Berntsen, T. K., Fuglestvedt, J. S., Joshi, M. M., Shine, K. P., Stuber, N., Ponater, M., Sausen, R., Hauglustaine, D. A., and Li, L.: Response of climate to regional emissions of ozone precursors: sensitivities and warming potentials, Tellus B, 57, 283–304, 2005.

Borken, J., Steller, H., Meretei, T., and Vanhove, F.: Global and country inventory of road passenger and freight transportation – fuel consumption and emissions of air pollutants in year 2000, Transport Res. Rec., 2011, 127–136, doi:10.3141/2011-14, 2007.

Brasseur, G. P., Muller, J. F., and Granier, C.: Atmospheric impact of NO_x emissions by subsonic aircraft: a three-dimensional model study, J. Geophys. Res.-Atmos., 101, 1423–1428, 1996.

Carver, G. D. and Stott, P. A.: IMPACT: an implicit time integration scheme for chemical species and families, Ann. Geophys.-Atm. Hydr., 18, 337–346, 2000.

Carver, G. D., Brown, P. D., and Wild, O.: The ASAD atmospheric chemistry integration package and chemical reaction database, Comput. Phys. Commun., 105, 197–215, 1997.

Corbett, J. J. and Koehler, H. W.: Updated emissions from ocean shipping, J. Geophys. Res.-Atmos., 108(D20), 4650, doi:10.1029/2003jd003751, 2003.

Crutzen, P. J.: Role of the tropics in atmospheric chemistry, in: The Geophysiology of Amazonia, edited by: Dickinson, R. E., John Wiley, New York, 107–130, 1987.

Dalsøren, S. B. and Isaksen, I. S. A.: CTM study of changes in tropospheric hydroxyl distribution 1990–2001 and its impact on methane, Geophys. Res. Lett., 33(7), L23811, doi:10.1029/2006gl027295, 2006.

ACPD
11, 16801–16859, 2011

Dalsøren, S. B., Eide, M. S., Endresen, Ø., Mjelde, A., Gravir, G., and Isaksen, I. S. A.: Update on emissions and environmental impacts from the international fleet of ships: the contribution from major ship types and ports, Atmos. Chem. Phys., 9, 2171–2194, doi:10.5194/acp-9-2171-2009, 2009.

Dalsøren, S. B., Eide, M. S., Myhre, G., Endresen, O., Isaksen, I. S. A., and Fuglestvedt, J. S.: Impacts of the large increase in international ship traffic 2000–2007 on tropospheric ozone and methane, Environ. Sci. Technol., 44, 2482–2489, doi:10.1021/es902628e, 2010.

Danilin, M. Y., Fahey, D. W., Schumann, U., Prather, M. J., Penner, J. E., Ko, M. K. W., Weisenstein, D. K., Jackman, C. H., Pitari, G., Kohler, I., Sausen, R., Weaver, C. J., Douglass, A. R., Connell, P. S., Kinnison, D. E., Dentener, F. J., Fleming, E. L., Berntsen, T. K., Isaksen, I. S. A., Haywood, J. M., and Karcher, B.: Aviation fuel tracer simulation: model intercomparison and implications, Geophys. Res. Lett., 25, 3947–3950, 1998.

Dentener, F., Peters, W., Krol, M., van Weele, M., Bergamaschi, P., and Lelieveld, J.: Interannual variability and trend of CH_4 lifetime as a measure for OH changes in the 1979–1993 time period, J. Geophys. Res.-Atmos., 108(D15), 4442, doi:10.1029/2002jd002916, 2003.

Duncan, B. N. and Logan, J. A.: Model analysis of the factors regulating the trends and variability of carbon monoxide between 1988 and 1997, Atmos. Chem. Phys., 8, 7389–7403, doi:10.5194/acp-8-7389-2008, 2008.

Eide, M. S., Endresen, O., Mjelde, A., Mangset, L. E., and Gravir, G.: Ship emissions of the future, Technical Report No 2007–1325, Det Norske Veritas, Høvik, Norway, 2007.

Emanuel, K. A.: A scheme for representing cumulus convection in large-scale models, J. Atmos. Sci., 48, 2313–2335, 1991.

Emanuel, K. A.: A cumulus representation based on the episodic mixing model: the importance of mixing and microphysics in predicting humidity, AMS Meteorol. Monogr., 24, 185–192, 1993.

Endresen, O., Sorgard, E., Sundet, J. K., Dalsøren, S. B., Isaksen, I. S. A., Berglen, T. F., and Gravir, G.: Emission from international sea transportation and environmental impact, J. Geophys. Res.-Atmos., 108(D17), 4560, doi:10.1029/2002jd002898, 2003.

Endresen, O., Sorgard, E., Behrens, H. L., Brett, P. O., and Isaksen, I. S. A.: A historical reconstruction of ships' fuel consumption and emissions, J. Geophys. Res.-Atmos., 112, D12301, doi:10.1029/2006jd007630, 2007.

Eyring, V., Kohler, H. W., Lauer, A., and Lemper, B.: Emissions from international shipping: 2. Impact of future technologies on scenarios until 2050, J. Geophys. Res.-Atmos., 110,

ACPD
11, 16801–16859, 2011

D17306, doi:10.1029/2004jd005620, 2005.
Eyring, V., Stevenson, D. S., Lauer, A., Dentener, F. J., Butler, T., Collins, W. J., Ellingsen, K., Gauss, M., Hauglustaine, D. A., Isaksen, I. S. A., Lawrence, M. G., Richter, A., Rodriguez, J. M., Sanderson, M., Strahan, S. E., Sudo, K., Szopa, S., van Noije, T. P. C., and Wild, O.: Multi-model simulations of the impact of international shipping on Atmospheric Chemistry and Climate in 2000 and 2030, Atmos. Chem. Phys., 7, 757–780, doi:10.5194/acp-7-757-2007, 2007.
Eyring, V., Isaksen, I. S. A., Berntsen, T., Collins, W. J., Corbett, J. J., Endresen, O., Grainger, R. G., Moldanova, J., Schlager, H., and Stevenson, D. S.: Transport impacts on atmosphere and climate: shipping, Atmos. Environ., 44, 4735–4771, doi:10.1016/j.atmosenv.2009.04.059, 2010.
Folberth, G. A., Hauglustaine, D. A., Lathière, J., and Brocheton, F.: Interactive chemistry in the Laboratoire de Météorologie Dynamique general circulation model: model description and impact analysis of biogenic hydrocarbons on tropospheric chemistry, Atmos. Chem. Phys., 6, 2273–2319, doi:10.5194/acp-6-2273-2006, 2006.
Fuglestvedt, J., Berntsen, T., Myhre, G., Rypdal, K., and Skeie, R. B.: Climate forcing from the transport sectors, Proc. Natl. Acad. Sci. USA, 105, 454–458, doi:10.1073/pnas.0702958104, 2008.
Gauss, M., Isaksen, I. S. A., Wong, S., and Wang, W. C.: Impact of H_2O emissions from cryoplanes and kerosene aircraft on the atmosphere, J. Geophys. Res.-Atmos., 108(D10), 4304, doi:10.1029/2002jd002623, 2003.
Gauss, M., Isaksen, I. S. A., Lee, D. S., and Søvde, O. A.: Impact of aircraft NO_x emissions on the atmosphere – tradeoffs to reduce the impact, Atmos. Chem. Phys., 6, 1529–1548, doi:10.5194/acp-6-1529-2006, 2006.
Grewe, V. and Stenke, A.: AirClim: an efficient tool for climate evaluation of aircraft technology, Atmos. Chem. Phys., 8, 4621–4639, doi:10.5194/acp-8-4621-2008, 2008.
Grewe, V., Dameris, M., Hein, R., Kohler, I., and Sausen, R.: Impact of future subsonic aircraft NO_x emissions on the atmospheric composition, Geophys. Res. Lett., 26, 47–50, 1999.
Grewe, V., Stenke, A., Ponater, M., Sausen, R., Pitari, G., Iachetti, D., Rogers, H., Dessens, O., Pyle, J., Isaksen, I. S. A., Gulstad, L., Søvde, O. A., Marizy, C., and Pascuillo, E.: Climate impact of supersonic air traffic: an approach to optimize a potential future supersonic fleet – results from the EU-project SCENIC, Atmos. Chem. Phys., 7, 5129–5145, doi:10.5194/acp-7-5129-2007, 2007.

ACPD
11, 16801–16859, 2011

Grewe, V., Tsati, E., and Hoor, P.: On the attribution of contributions of atmospheric trace gases to emissions in atmospheric model applications, Geosci. Model Dev., 3, 487–499, doi:10.5194/gmd-3-487-2010, 2010.

Grooss, J. U., Bruhl, C., and Peter, T.: Impact of aircraft emissions on tropospheric and stratospheric ozone. Part I: Chemistry and 2-D model results, Atmos. Environ., 32, 3173–3184, 1998.

Hansen, J., Sato, M., and Ruedy, R.: Radiative forcing and climate response, J. Geophys. Res.-Atmos., 102, 6831–6864, 1997.

Hauglustaine, D. A., Hourdin, F., Jourdain, L., Filiberti, M. A., Walters, S., Lamarque, J. F., and Holland, E. A.: Interactive chemistry in the Laboratoire de Meteorologie Dynamique general circulation model: description and background tropospheric chemistry evaluation, J. Geophys. Res.-Atmos., 109, D04314, doi:10.1029/2003jd003957, 2004.

Hesstvedt, E., Hov, O., and Isaksen, I. S. A.: Quasi-steady-state approximations in air pollution modeling – comparison of two numerical schemes for oxidant prediction, Int. J. Chem. Kinet., 10, 971–994, 1978.

Hidalgo, H. and Crutzen, P. J.: Tropospheric and stratospheric composition perturbed by NO_x emissions of high-altitude aircraft, J. Geophys. Res.-Oc. Atm., 82, 5833–5866, 1977.

Hoor, P., Borken-Kleefeld, J., Caro, D., Dessens, O., Endresen, O., Gauss, M., Grewe, V., Hauglustaine, D., Isaksen, I. S. A., Jöckel, P., Lelieveld, J., Myhre, G., Meijer, E., Olivie, D., Prather, M., Schnadt Poberaj, C., Shine, K. P., Staehelin, J., Tang, Q., van Aardenne, J., van Velthoven, P., and Sausen, R.: The impact of traffic emissions on atmospheric ozone and OH: results from QUANTIFY, Atmos. Chem. Phys., 9, 3113–3136, doi:10.5194/acp-9-3113-2009, 2009.

Hourdin, F. and Armengaud, A.: The use of finite-volume methods for atmospheric advection of trace species. Part I: Test of various formulations in a general circulation model, Mon. Weather Rev., 127, 822–837, 1999.

Houweling, S., Dentener, F., and Lelieveld, J.: The impact of nonmethane hydrocarbon compounds on tropospheric photochemistry, J. Geophys. Res.-Atmos., 103, 10673–10696, 1998.

Hsu, J., Prather, M. J., and Wild, O.: Diagnosing the stratosphere-to-troposphere flux of ozone in a chemistry transport model, J. Geophys. Res.-Atmos., 110, D19305, doi:10.1029/2005jd006045, 2005.

IPCC: Aviation and the Global Atmosphere, edited by: Penner, J. E., Lister, D. H., Griggs, D. J.,

ACPD
11, 16801–16859, 2011

Dokken, D. J., and McFarland, M., Cambridge University Press, Cambridge, United Kingdom and New York, NY, USA, 1999.
IPCC: Climate Change 2001: The Scientific Basis. Contribution of Working Group I to the Third Assessment Report of the Intergovernmental Panel on Climate Change, edited by: Houghton, J. T., Ding, Y., Griggs, D. J., Noguer, M., van der Linden, P. J., Dai, X., Maskell, K., and Johnson, C. A., Cambridge University Press, Cambridge, UK and New York, NY, USA, 881 pp., 2001.
Isaksen, I. S. A. and Dalsøren, S. B.: Getting a better estimate of an atmospheric radical, Science, 331(6013), 38–39, doi:10.1126/science.1199773, 2011.
Isaksen, I. S. A., Zerefos, C., Kourtidis, K., Meleti, C., Dalsøren, S. B., Sundet, J. K., Grini, A., Zanis, P., and Balis, D.: Tropospheric ozone changes at unpolluted and semipolluted regions induced by stratospheric ozone changes, J. Geophys. Res.-Atmos., 110, D02302, doi:10.1029/2004jd004618, 2005.
Jöckel, P., Tost, H., Pozzer, A., Brühl, C., Buchholz, J., Ganzeveld, L., Hoor, P., Kerkweg, A., Lawrence, M. G., Sander, R., Steil, B., Stiller, G., Tanarhte, M., Taraborrelli, D., van Aardenne, J., and Lelieveld, J.: The atmospheric chemistry general circulation model ECHAM5/MESSy1: consistent simulation of ozone from the surface to the mesosphere, Atmos. Chem. Phys., 6, 5067–5104, doi:10.5194/acp-6-5067-2006, 2006.
Johnson, C., Henshaw, J., and McInnes, G.: Impact of aircraft and surface emissions of nitrogen-oxides on tropospheric ozone and global warming, Nature, 355, 69–71, 1992.
Koffi, B., Szopa, S., Cozic, A., Hauglustaine, D., and van Velthoven, P.: Present and future impact of aircraft, road traffic and shipping emissions on global tropospheric ozone, Atmos. Chem. Phys., 10, 11681–11705, doi:10.5194/acp-10-11681-2010, 2010.
Kraabøl, A. G., Berntsen, T. K., Sundet, J. K., and Stordal, F.: Impacts of NO_x emissions from subsonic aircraft in a global three-dimensional chemistry transport model including plume processes, J. Geophys. Res.-Atmos., 107(D22), 4655, doi:10.1029/2001jd001019, 2002.
Lacis, A. A., Wuebbles, D. J., and Logan, J. A.: Radiative forcing of climate by changes in the vertical-distribution of ozone, J. Geophys. Res.-Atmos., 95, 9971–9981, 1990.
Law, K. S., Plantevin, P. H., Shallcross, D. E., Rogers, H. L., Pyle, J. A., Grouhel, C., Thouret, V., and Marenco, A.: Evaluation of modeled O-3 using measurement of ozone by airbus in-service aircraft (MOZAIC) data, J. Geophys. Res.-Atmos., 103, 25721–25737, 1998.
Law, K. S., Plantevin, P. H., Thouret, V., Marenco, A., Asman, W. A. H., Lawrence, M., Crutzen, P. J., Muller, J. F., Hauglustaine, D. A., and Kanakidou, M.: Comparison between

ACPD
11, 16801–16859, 2011

global chemistry transport model results and measurement of ozone and water vapor by airbus in-service aircraft (MOZAIC) data, J. Geophys. Res.-Atmos., 105, 1503–1525, 2000.
Lawrence, M. G. and Crutzen, P. J.: Influence of NO_x emissions from ships on tropospheric photochemistry and climate, Nature, 402, 167–170, 1999.
Le Treut, H., Forichon, M., Boucher, O., and Li, Z. X.: Sulfate aerosol indirect effect and CO_2 greenhouse forcing: equilibrium response of the LMD GCM and associated cloud feedbacks, J. Climate, 11, 1673–1684, 1998.
Lee, D. S., Fahey, D. W., Forster, P. M., Newton, P. J., Wit, R. C. N., Lim, L. L., Owen, B., and Sausen, R.: Aviation and global climate change in the 21st century, Atmos. Environ., 43, 3520–3537, doi:10.1016/j.atmosenv.2009.04.024, 2009.
Lee, D. S., Pitari, G., Grewe, V., Gierens, K., Penner, J. E., Petzold, A., Prather, M. J., Schumann, U., Bais, A., Berntsen, T., Iachetti, D., Lim, L. L., and Sausen, R.: Transport impacts on atmosphere and climate: aviation, Atmos. Environ., 44, 4678–4734, doi:10.1016/j.atmosenv.2009.06.005, 2010.
Lelieveld, J., Peters, W., Dentener, F. J., and Krol, M. C.: Stability of tropospheric hydroxyl chemistry, J. Geophys. Res.-Atmos., 107(D23), 4715, doi:10.1029/2002jd002272, 2002.
Lelieveld, J., Brenninkmeijer, C. A. M., Joeckel, P., Isaksen, I. S. A., Krol, M. C., Mak, J. E., Dlugokencky, E., Montzka, S. A., Novelli, P. C., Peters, W., and Tans, P. P.: New directions: watching over tropospheric hydroxyl (OH), Atmos. Environ., 40, 5741–5743, doi:10.1016/j.atmosenv.2006.04.008, 2006.
Meijer, E. W., van Velthoven, P. F. J., Brunner, D. W., Huntrieser, H., and Kelder, H.: Improvement and evaluation of the parameterisation of nitrogen oxide production by lightning, Phys. Chem. Earth Pt. C, 26, 577–583, 2001.
Montzka, S. A., Krol, M., Dlugokencky, E., Hall, B., Jöckel, P., and Lelieveld, J.: Small interannual variability of global atmospheric hydroxyl, Science, 331(6013), 67–69, doi:10.1126/science.1197640, 2011.
Myhre, G., Karlsdottir, S., Isaksen, I. S. A., and Stordal, F.: Radiative forcing due to changes in tropospheric ozone in the period 1980 to 1996, J. Geophys. Res.-Atmos., 105, 28935–28942, 2000.
Myhre, G., Nilsen, J. S., Gulstad, L., Shine, K. P., Rognerud, B., and Isaksen, I. S. A.: Radiative forcing due to stratospheric water vapour from CH_4 oxidation, Geophys. Res. Lett., 34, L01807, doi:10.1029/2006gl027472, 2007.
Myhre, G., Shine, K. P., Rädel, G., Gauss, M., Isaksen, I. S. A., Tang, Q., Prather, M. J.,

ACPD
11, 16801–16859, 2011

Williams, J. E., van Velthoven, P., Dessens, O., Koffi, B., Szopa, S., Hoor, P., Grewe, V., Borken-Kleefeld, J., Berntsen, T. K., and Fuglestvedt, J. S.: Radiative forcing due to changes in ozone and methane caused by the transport sector, Atmos. Environ., 45, 387–394, doi:10.1016/j.atmosenv.2010.10.001, 2011.

Nakicenovic, N., Davidson, O., Davis, G., Grübler, A., Kram, T., La Rovere, E. L., Metz, B., Morita, T., Pepper, W., Pitcher, H., Sankovski, A., Shukla, P., Swart, R., Watson, R., and Dadi, Z.: Special Report on Emissions Scenarios, Cambridge University Press, Cambridge, 599 pp., 2000.

O'Connor, F. M., Carver, G. D., Savage, N. H., Pyle, J. A., Methven, J., Arnold, S. R., Dewey, K., and Kent, J.: Comparison and visualisation of high-resolution transport modelling with aircraft measurements, Atmos. Sci. Lett., 6, 164–170, doi:10.1002/asl.111, 2005.

Olivier, J. G. J., Van Aardenne, J. A., Dentener, F., Ganzeveld, L., and Peters, J. A. H. W.: Recent trends in global greenhouse gas emissions: regional trends and spatial distribution of key sources, in: Non-CO_2 Greenhouse Gases (NCGG-4), Millpress, Rotterdam, 325–330, 2005.

Owen, B., Lee, D. S., and Lim, L.: Flying into the future: aviation emissions scenarios to 2050, Environ. Sci. Technol., 44, 2255–2260, doi:10.1021/es902530z, 2010.

Prather, M. J.: Numerical advection by conservation of 2nd-order moments, J. Geophys. Res.-Atmos., 91, 6671–6681, 1986.

Prather, M. J. and Hsu, J.: Coupling of nitrous oxide and methane by global atmospheric chemistry, Science, 330, 952–954, doi:10.1126/science.1196285, 2010.

Prather, M. J., Zhu, X., Tang, Q., Hsu, J., and Neu, J. L.: An atmospheric chemist in search of the tropopause, J. Geophys. Res., 116, D04306, doi:10.1029/2010JD014939, 2011.

Price, C. and Rind, D.: A simple lightning parameterization for calculating global lightning distributions, J. Geophys. Res.-Atmos., 97, 9919–9933, 1992.

Ramanathan, V. and Dickinson, R. E.: Role of stratospheric ozone in the zonal and seasonal radiative energy-balance of the Earth-troposphere system, J. Atmos. Sci., 36, 1084–1104, 1979.

Rogers, H., Teyssèdre, H., Pitari, G., Grewe, V., van Velthoven, P., and Sundet, J.: Model intercomparison of the transport of aircraft-like emissions from sub- and supersonic aircraft, Meteorol. Z., 11, 151–159, doi:10.1127/0941-2948/2002/0011-0151, 2002.

Russell, G. L. and Lerner, J. A.: A new finite-differencing scheme for the tracer transport-equation, J. Appl. Meteorol., 20, 1483–1498, 1981.

ACPD
11, 16801–16859, 2011

Sander, S. P., Orkin, V. L., Kurylo, M. J., Golden, D. M., Barker, J. R., Huie, R. E., Kolb, C. E., Abbatt, J. P. D., Friedl, R. R., Burkholder, J. B., Moortgat, G. K., and Wine, P. H.: Chemical kinetics and photochemical data for use in atmospheric studies, JPL Publication 06–2, NASA/JPL, Jet Propulsion Laboratory, California Institute of Technology, Pasadena, California, Evaluation Number 15, 2006.

Sausen, R., Isaksen, I., Grewe, V., Hauglustaine, D., Lee, D. S., Myhre, G., Kohler, M. O., Pitari, G., Schumann, U., Stordal, F., and Zerefos, C.: Aviation radiative forcing in 2000: an update on IPCC (1999), Meteorol. Z., 14, 555–561, doi:10.1127/0941-2948/2005/0049, 2005.

Savage, N. H., Law, K. S., Pyle, J. A., Richter, A., Nüß, H., and Burrows, J. P.: Using GOME NO_2 satellite data to examine regional differences in TOMCAT model performance, Atmos. Chem. Phys., 4, 1895–1912, doi:10.5194/acp-4-1895-2004, 2004.

Schnadt Poberaj, C., Staehelin, J., Bintania, R., van Velthoven, P., Dessens, O., Gauss, M., Isaksen, I. S. A., Grewe, V., Jöckel, P., Hoor, P., Koffi, B., Hauglustaine, D., and Olivié, D.: QUANTIFY model evaluation of global chemistry models: carbon monoxide, in: Proceedings of the 2nd International Conference on Transport, Atmosphere and Climate, DLR Forschungsbericht 2010-10, ISSN 1434-8454,163–168, 2010.

Schumann, U.: The impact of nitrogen oxides emissions from aircraft upon the atmosphere at flight altitudes – results from the AERONOX project, Atmos. Environ., 31, 1723–1733, 1997.

Schumann, U. and Huntrieser, H.: The global lightning-induced nitrogen oxides source, Atmos. Chem. Phys., 7, 3823–3907, doi:10.5194/acp-7-3823-2007, 2007.

Schumann, U., Schlager, H., Arnold, F., Ovarlez, J., Kelder, H., Hov, O., Hayman, G., Isaksen, I. S. A., Staehelin, J., and Whitefield, P. D.: Pollution from aircraft emissions in the North Atlantic flight corridor: overview on the POLINAT projects, J. Geophys. Res.-Atmos., 105, 3605–3631, 2000.

Shindell, D. T., Faluvegi, G., Bell, N., and Schmidt, G. A.: An emissions-based view of climate forcing by methane and tropospheric ozone, Geophys. Res. Lett., 32, L04803, doi:10.1029/2004gl021900, 2005.

Skeie, R. B., Fuglestvedt, J., Berntsen, T., Lund, M. T., Myhre, G., and Rypdal, K.: Global temperature change from the transport sectors: historical development and future scenarios, Atmos. Environ., 43, 6260–6270, doi:10.1016/j.atmosenv.2009.05.025, 2009.

Søvde, O. A., Gauss, M., Isaksen, I. S. A., Pitari, G., and Marizy, C.: Aircraft pollution – a futuristic view, Atmos. Chem. Phys., 7, 3621–3632, doi:10.5194/acp-7-3621-2007, 2007.

ACPD
11, 16801–16859, 2011

Søvde, O. A., Gauss, M., Smyshlyaev, S. P., and Isaksen, I. S. A.: Evaluation of the chemical transport model Oslo CTM2 with focus on arctic winter ozone depletion, J. Geophys. Res.-Atmos., 113, D09304, doi:10.1029/2007jd009240, 2008.

Stevenson, D. S., Doherty, R. M., Sanderson, M. G., Collins, W. J., Johnson, C. E., and Derwent, R. G.: Radiative forcing from aircraft NO_x emissions: mechanisms and seasonal dependence, J. Geophys. Res.-Atmos., 109, D17307, doi:10.1029/2004jd004759, 2004.

Tang, Q. and Prather, M. J.: Correlating tropospheric column ozone with tropopause folds: the Aura-OMI satellite data, Atmos. Chem. Phys., 10, 9681–9688, doi:10.5194/acp-10-9681-2010, 2010.

Tang, Q., Prather, M. J., and Hsu, J.: Stratosphere-troposphere exchange ozone flux related to deep convection, Geophys. Res. Lett., 38, L03806, doi:10.1029/2010gl046039, 2011.

Teyssèdre, H., Michou, M., Clark, H. L., Josse, B., Karcher, F., Olivié, D., Peuch, V.-H., Saint-Martin, D., Cariolle, D., Attié, J.-L., Nédélec, P., Ricaud, P., Thouret, V., van der A, R. J., Volz-Thomas, A., and Chéroux, F.: A new tropospheric and stratospheric Chemistry and Transport Model MOCAGE-Climat for multi-year studies: evaluation of the present-day climatology and sensitivity to surface processes, Atmos. Chem. Phys., 7, 5815–5860, doi:10.5194/acp-7-5815-2007, 2007.

Tiedtke, M.: A comprehensive mass flux scheme for cumulus parameterization in large-scale models, Mon. Weather Rev., 117, 1779–1800, 1989.

Uherek, E., Halenka, T., Borken-Kleefeld, J., Balkanski, Y., Berntsen, T., Borrego, C., Gauss, M., Hoor, P., Juda-Rezler, K., Lelieveld, J., Melas, D., Rypdal, K., and Schmid, S.: Transport impacts on atmosphere and climate: land transport, Atmos. Environ., 44, 4772–4816, doi:10.1016/j.atmosenv.2010.01.002, 2010.

Van Leer, B.: Towards the ultimate conservative difference scheme. IV. A new approach to numerical convection, J. Comput. Phys., 23, 276–299, doi:10.1016/0021-9991(77)90095-x, 1977.

Wang, W. C. and Sze, N. D.: Coupled effects of atmospheric N_2O and O_3 on the Earth's climate, Nature, 286, 589–590, 1980.

van der Werf, G. R., Randerson, J. T., Giglio, L., Collatz, G. J., Kasibhatla, P. S., and Arellano Jr., A. F.: Interannual variability in global biomass burning emissions from 1997 to 2004, Atmos. Chem. Phys., 6, 3423–3441, doi:10.5194/acp-6-3423-2006, 2006.

Wild, O., Zhu, X., and Prather, M. J.: Fast-j: Accurate simulation of in- and below-cloud photolysis in tropospheric chemical models, J. Atmos. Chem., 37, 245–282, 2000.

ACPD
11, 16801–16859, 2011

Wild, O., Sundet, J. K., Prather, M. J., Isaksen, I. S. A., Akimoto, H., Browell, E. V., and Oltmans, S. J.: Chemical transport model ozone simulations for spring 2001 over the Western Pacific: comparisons with TRACE-P lidar, ozonesondes, and total ozone mapping spectrometer columns, J. Geophys. Res.-Atmos., 108(D21), 8826, doi:10.1029/2002jd003283, 2003.

Williams, J. E. and van Noije, T. P. C.: On the updating of the modified Carbon Bond Mechanism IV for use in global Chemistry Transport Models, KNMI Scientific Report WR 2008-02, 64 pp., De Bilt, The Netherlands, 2008.

Williams, J. E., Scheele, M. P., van Velthoven, P. F. J., Thouret, V., Saunois, M., Reeves, C. E., and Cammas, J.-P.: The influence of biomass burning and transport on tropospheric composition over the tropical Atlantic Ocean and Equatorial Africa during the West African monsoon in 2006, Atmos. Chem. Phys., 10, 9797–9817, doi:10.5194/acp-10-9797-2010, 2010.

Williamson, D. L. and Rasch, P. J.: Two-dimensional semi-lagrangian transport with shape-preserving interpolation, Mon. Weather Rev., 117, 102–129, 1989.

ACPD
11, 16801–16859, 2011

Table 1. Global annual emissions of NO_x, CO and NMHC provided by QUANTIFY (http://www.ip-quantify.eu) for the years 2000, 2025 and 2050 in the B1 scenario. The 2000 emissions are from the final QUANTIFY dataset and thereby differ from the preliminary emissions used in Hoor et al. (2009).

	NO_x emissions in Tg(N)			CO emissions in Tg(C)			NMHC emissions in Tg(C)[b]		
Source	2000	2025B1	2050B1	2000	2025B1	2050B1	2000	2025B1	2050B1
Aircraft	0.85	1.18/1.13[a]	1.04/0.79[a]	–	–	–	–	–	–
Ship	4.39	4.93	5.05	0.6	1.0	1.5	0.26	0.38	0.48
Road	9.09	3.29	0.51	47.2	14.8	1.7	8.76	2.08	0.41
Non-traffic	28.0	30.8	31.3	341.4	220.5	196.5	76.51	78.48	82.33
Biogenic, soil	6.89	6.89	6.89	48.2	48.2	48.2	340.5	340.5	340.5

[a] B1 ACARE aircraft emissions.
[b] A factor of 161/210 was used to convert from Tg(NMHC) to Tg(C), see Table 4.7b in IPCC (2001).

ACPD
11, 16801–16859, 2011

Table 2. Specifications of the participating models in this study (modified from Hoor et al., 2009).

Model	TM4	p-TOMCAT	OsloCTM2	LMDz-INCA	UCI CTM	MOCAGE
Operated	KNMI	UCAM-DCHEM	UiO	LSCE	UCI	Météo-France
Model type	CTM	CTM	CTM	CCM (nudged)	CTM	CTM
Meteorology	ECMWF OD	ECMWF OD	ECMWF OD	ECMWF OD	ECMWF OD	ECMWF OD
Hor. resolution	$2^\circ \times 3^\circ$	T21	T42	$3.75^\circ \times 2.5^\circ$	T42	T21
Levels	34	31	60	19	40	60
Model top (hPa)	0.1	10	0.1	3	2	0.1
Transport scheme	Russell and Lerner (1981)	Prather (1986)	Prather (1986)	van Leer (1977)	Prather (1986)	Williamson and Rasch (1989)
Convection	Tiedtke (1989)	Tiedtke (1989)	Tiedtke (1989)	Emanuel (1991, 1993)	Tiedtke (1989)	Bechtold et al. (2001)
Lightning	Meijer et al. (2001)	Price and Rind (1992)	Price and Rind (1992)	Price and Rind (1992), modified	Price and Rind (1992)	Climatology
Transp. species	26	35	76	66	28	65
Total species	42	51	98	96	38	82
Gas phase reactions	68 + 16	112 + 27	163 + 47	291 + 51	90 + 22	186 + 47
Het. Reactions	2	1	7	4	0	9
Strat. chemistry	no	no	yes	no	LINOZ	yes
NMHC chemistry	yes, CBM4	yes	yes	yes	yes	yes
Lightning NO_x ($TgN\,yr^{-1}$)	5	5	5	2	5	5
References	Williams et al. (2010)	O'Connor et al. (2005)	Gauss et al. (2003), Søvde et al. (2008)	Hauglustaine et al. (2004), Folberth et al. (2006)	Wild et al. (2003), Hsu et al. (2005)	Teyssèdre et al. (2007)

ACPD
11, 16801–16859, 2011

Table 3. Global annual average of the change in O_3 molecules per NO_x molecule emitted from aviation and shipping, given as ensemble means and standard deviations.

	2000	2025B1	2050B1	2025B1ACARE	2050B1ACARE
AIR	2.05 (±0.51)	1.90 (±0.42)	2.16 (±0.52)	1.95 (±0.42)	2.31 (±0.59)
SHIP	0.509 (±0.185)	0.508 (±0.185)	0.535 (±0.194)	–	–

ACPD
11, 16801–16859, 2011

Table 4. Relative changes (%) in methane lifetimes (integrated up to 50 hPa) due to a 5 % decrease in traffic emissions. Values are given relative to the BASE case, and are scaled to 100 % by multiplying with 20. Both the mean of the six models and the standard deviations (indicating the spread of the models) are given. Note that this table does not include the feedback effect of methane changes on its own lifetime.

	AIR	SHIP
2000	1.30 (±0.30)	3.68 (±0.47)
2025B1	1.69 (±0.35)	3.73 (±0.40)
2050B1	1.68 (±0.38)	3.92 (±0.48)
2025B1ACARE	1.59 (±0.34)	–
2050B1ACARE	1.17 (±0.28)	–

ACPD
11, 16801–16859, 2011

Table 5. Radiative forcings (m W m^{-2}) from changes in ozone, methane (including stratospheric water vapour), and methane-induced ozone for different transport sectors and years/scenarios given as ensemble means and standard deviations. Note that the history of emissions has been taken into account, and that the fully scaled perturbations were used.

	AIRCRAFT				SHIPPING			
	O_3	CH_4	$O_{3(CH_4)}$	total	O_3	CH_4	$O_{3(CH_4)}$	total
2025B1	25.7 (±8.3)	−16.0 (±3.4)	−5.9 (±1.2)	3.8 (±6.1)	23.6 (±8.4)	−37.8 (±4.1)	−13.8 (±1.5)	−28.0 (±5.1)
2050B1	26.2 (±9.0)	−17.8 (±4.0)	−6.5 (±1.5)	1.9 (±6.4)	25.2 (±9.6)	−41.0 (±5.0)	−15.0 (±1.8)	−30.8 (±4.8)
2025B1ACARE	24.1 (±7.7)	−15.5 (±3.3)	−5.7 (±1.2)	2.9 (±5.8)	–	–	–	–
2050B1ACARE	18.9 (±6.8)	−14.3 (±3.4)	−5.2 (±1.2)	−0.6 (±4.6)	–	–	–	–

ACPD
11, 16801–16859, 2011

Table A1. Relative changes (%) in methane lifetimes (integrated up to 50 hPa) due to a 5 % decrease in aircraft emissions. Values are given relative to the BASE case, and are scaled to 100 % by multiplying with 20. Note that this table does not include the feedback effect of methane changes on its own lifetime.

	TM4	p-TOMCAT	OsloCTM2	LMDz-INCA	UCI CTM	MOCAGE
2000	1.27	1.61	0.85	1.07	1.60	1.41
2025B1	1.82	2.03	1.11	1.40	1.93	1.84
2050B1	1.77	2.04	1.09	1.37	2.04	1.78
2025B1ACARE	1.71	1.93	1.05	1.32	1.82	1.73
2050B1ACARE	1.22	1.47	0.75	0.94	1.43	1.23

ACPD
11, 16801–16859, 2011

Table A2. Same as Table A1, but due to a 5 % decrease in ship emissions.

	TM4	p-TOMCAT	OsloCTM2	LMDz-INCA	UCI CTM	MOCAGE
2000	4.17	3.44	3.77	3.20	4.28	3.24
2025B1	4.20	3.49	3.96	3.36	4.08	3.27
2050B1	4.38	3.56	4.14	3.51	4.52	3.43

ACPD
11, 16801–16859, 2011

Table A3. Radiative forcings ($mW\,m^{-2}$) from changes in ozone, methane (including stratospheric water vapour), and methane-induced ozone for different years/scenarios, due to emissions from aircraft. Note that the history of emissions has been taken into account, and that the fully scaled perturbations were used.

	TM4				p-TOMCAT				OsloCTM2			
	O_3	CH_4	$O_{3(CH_4)}$	total	O_3	CH_4	$O_{3(CH_4)}$	total	O_3	CH_4	$O_{3(CH_4)}$	total
2025B1	19.8	−17.3	−6.3	−3.8	40.1	−19.3	−7.0	13.8	20.6	−10.6	−3.9	6.2
2050B1	21.1	−18.8	−6.9	−4.5	42.7	−21.6	−7.9	13.2	20.4	−11.5	−4.2	4.7
2025B1ACARE	18.7	−16.6	−6.1	−4.0	38.2	−18.8	−6.9	12.6	20.3	−10.2	−3.7	6.4
2050B1ACARE	15.1	−14.8	−5.4	−5.2	31.4	−17.8	−6.5	7.1	14.6	−9.1	−3.3	2.1
	LMDz-INCA				UCI CTM				MOCAGE			
	O_3	CH_4	$O_{3(CH_4)}$	total	O_3	CH_4	$O_{3(CH_4)}$	total	O_3	CH_4	$O_{3(CH_4)}$	total
2025B1	18.0	−13.3	−4.9	−0.2	26.6	−18.3	−6.7	1.6	29.2	−17.5	−6.4	5.4
2050B1	18.0	−14.5	−5.3	−1.8	28.1	−21.6	−7.9	−1.4	27.2	−18.9	−6.9	1.4
2025B1ACARE	16.9	−12.8	−4.7	−0.6	25.1	−17.7	−6.5	0.9	25.5	−16.8	−6.1	2.5
2050B1ACARE	12.5	−11.4	−4.2	−3.1	19.9	−17.4	−6.4	−3.8	20.1	−14.9	−5.5	−0.3

ACPD
11, 16801–16859, 2011

Table A4. Same as Table A3, but due to emissions from shipping.

	TM4				p-TOMCAT				OsloCTM2			
	O_3	CH_4	$O_{3(CH_4)}$	total	O_3	CH_4	$O_{3(CH_4)}$	total	O_3	CH_4	$O_{3(CH_4)}$	total
2025B1	23.6	−42.6	−15.6	−34.6	19.2	−35.5	−13.0	−29.2	33.9	−40.2	−14.7	−21.0
2050B1	26.9	−45.7	−16.7	−35.5	20.0	−37.2	−13.6	−30.8	35.5	−43.2	−15.8	−23.5
	LMDz-INCA				UCI CTM				MOCAGE			
	O_3	CH_4	$O_{3(CH_4)}$	total	O_3	CH_4	$O_{3(CH_4)}$	total	O_3	CH_4	$O_{3(CH_4)}$	total
2025B1	18.6	−34.1	−12.4	−28.0	33.3	−41.5	−15.2	−23.4	13.3	−33.2	−12.1	−32.0
2050B1	19.6	−36.7	−13.4	−30.4	36.6	−47.2	−17.3	−27.9	12.5	−35.9	−13.1	−36.5

ACPD
11, 16801–16859, 2011

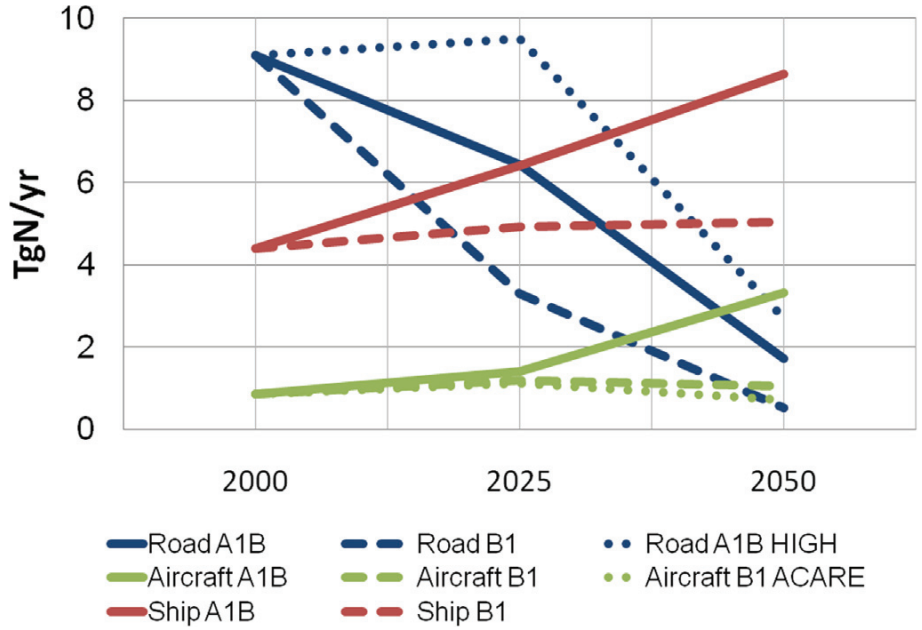

Fig. 1. Time development of NO_x emissions from different transport sectors in the SRES A1B and B1 scenarios, together with the alternative scenarios B1 ACARE and A1B HIGH (unit: $TgN\,yr^{-1}$).

ACPD
11, 16801–16859, 2011

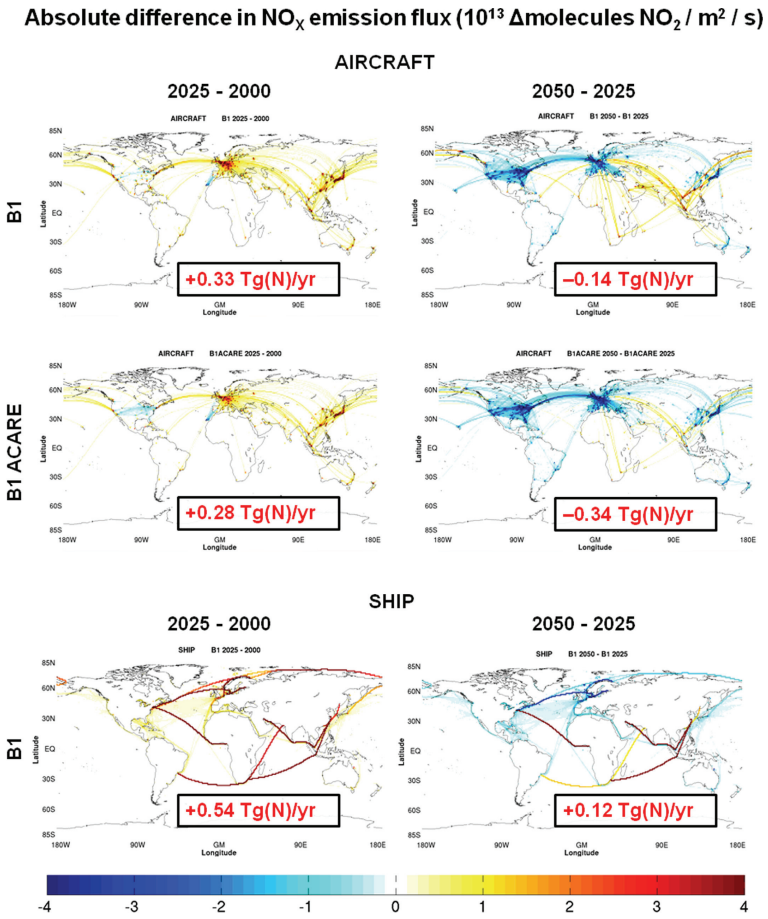

Fig. 2. Spatial distribution of the absolute difference in NO_x emission flux from aircraft and shipping for the B1 and B1 ACARE (only aircraft) scenarios (unit: 10^{13} Δmolecules NO_2 m^{-2} sm^{-1}) used in QUANTIFY.

ACPD
11, 16801–16859, 2011

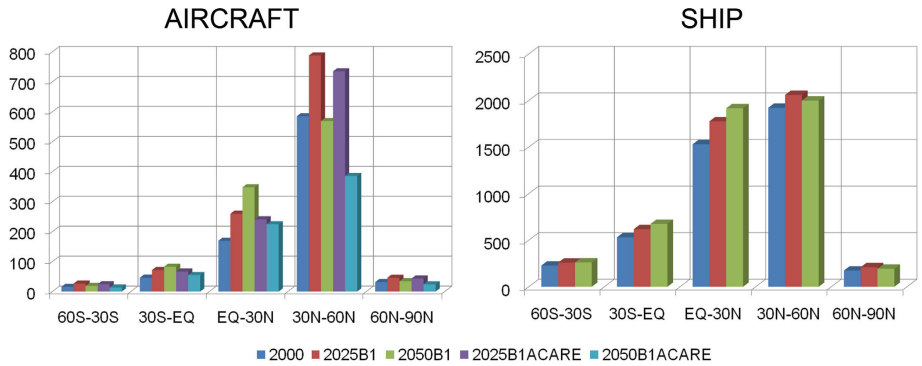

Fig. 3. NO_x emissions ($Gg(N)\,yr^{-1}$) from aircraft (left) and shipping (right) for different latitude intervals and for different years/scenarios. Note that 90° S–60° S is not shown in the figures because the emissions in this region are close to zero.

ACPD
11, 16801–16859, 2011

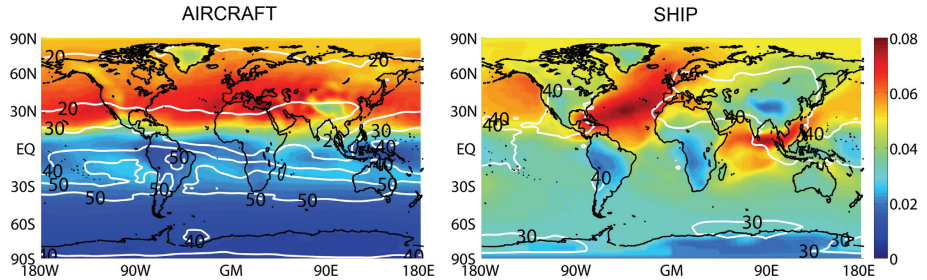

Fig. 4. Yearly mean perturbations of the ozone column (ΔDU, up to 40 hPa) due to a 5 % perturbation of aircraft emissions (left) and ship emissions (right) for the 2050 B1 scenario. The white contour lines show the standard deviation relative to the ensemble mean column perturbation (%), and have been smoothed to improve readability.

ACPD
11, 16801–16859, 2011

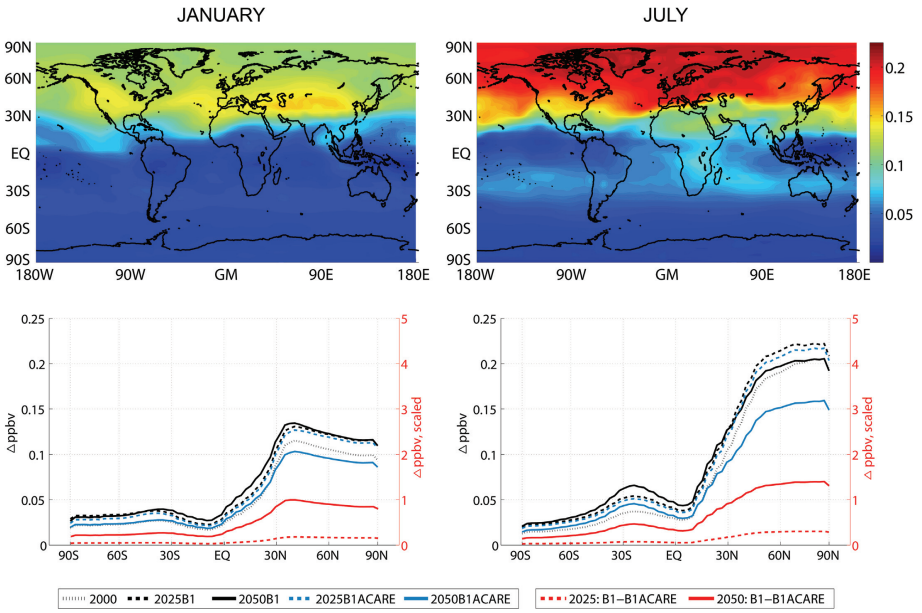

Fig. 5. Mean perturbations of ozone (Δppbv) in the upper troposphere (300–200 hPa) during January (left) and July (right) for the 2050 B1 scenario (top) and as zonal means for all scenarios (bottom). The color bar and the left *y*-axis show the unscaled impact of the 5 % perturbation of aircraft emissions (simulations BASE–AIR), while the red scales in the bottom figures are scaled up by a factor 20 from 5 % to 100 %.

ACPD
11, 16801–16859, 2011

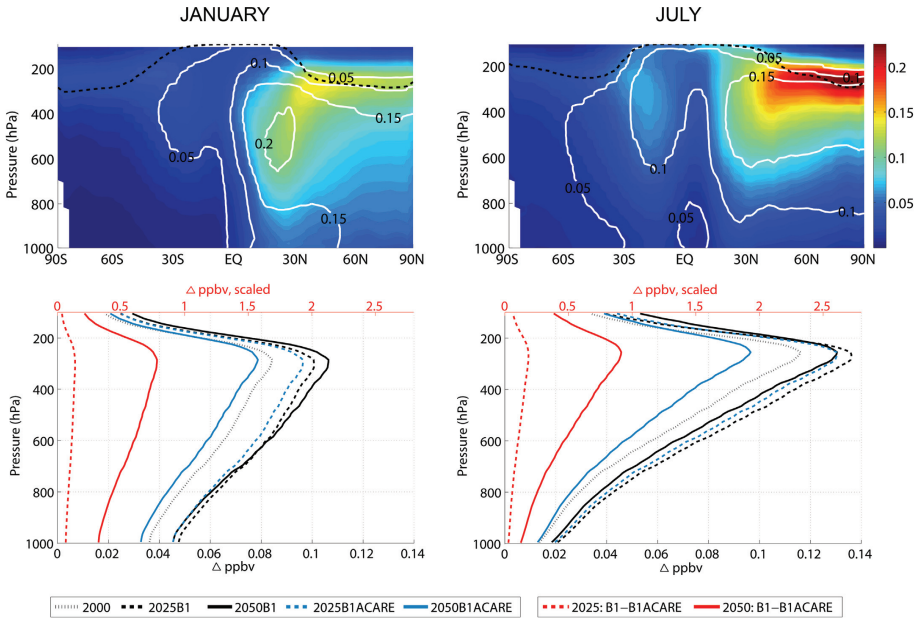

Fig. 6. Zonal mean perturbations of ozone (Δppbv) during January (left) and July (right) for the 2050 B1 scenario (top) and as Northern Hemisphere average for all years (bottom). In the top figures, solid contour lines show the change relative to the BASE simulation while the dashed line indicates the tropopause. The color bar and the bottom *x*-axis show the unscaled impact of the 5 % perturbation of aircraft emissions (simulations BASE–AIR), while the red scales in the bottom figures are scaled up by a factor 20 from 5 % to 100 %.

ACPD
11, 16801–16859, 2011

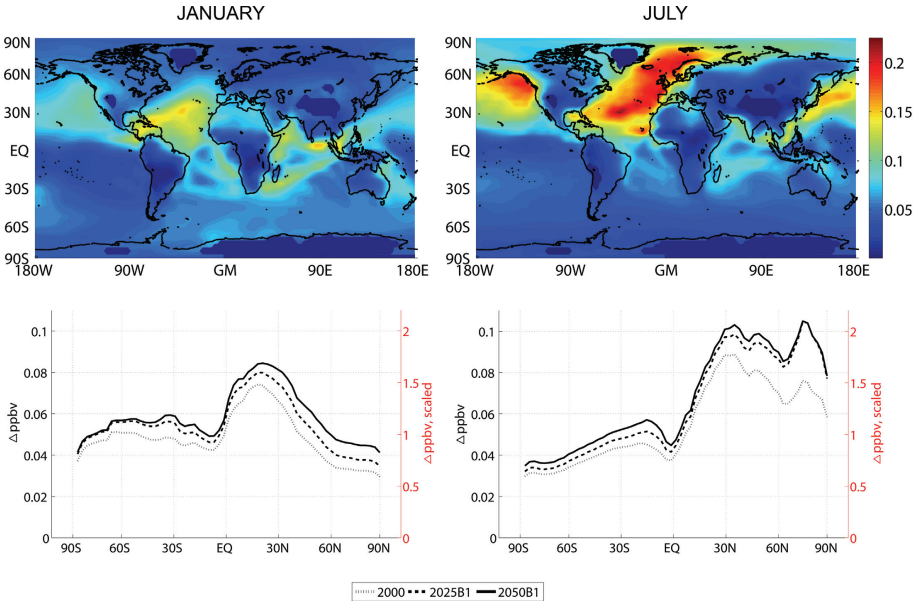

Fig. 7. Mean perturbations of ozone (Δppbv) in the lower troposphere (> 800 hPa) during January (left) and July (right) for the 2050 B1 scenario (top) and as zonal means for all years (bottom). The figures show the impact caused by a 5 % perturbation of ship emissions (simulations BASE–SHIP).

ACPD
11, 16801–16859, 2011

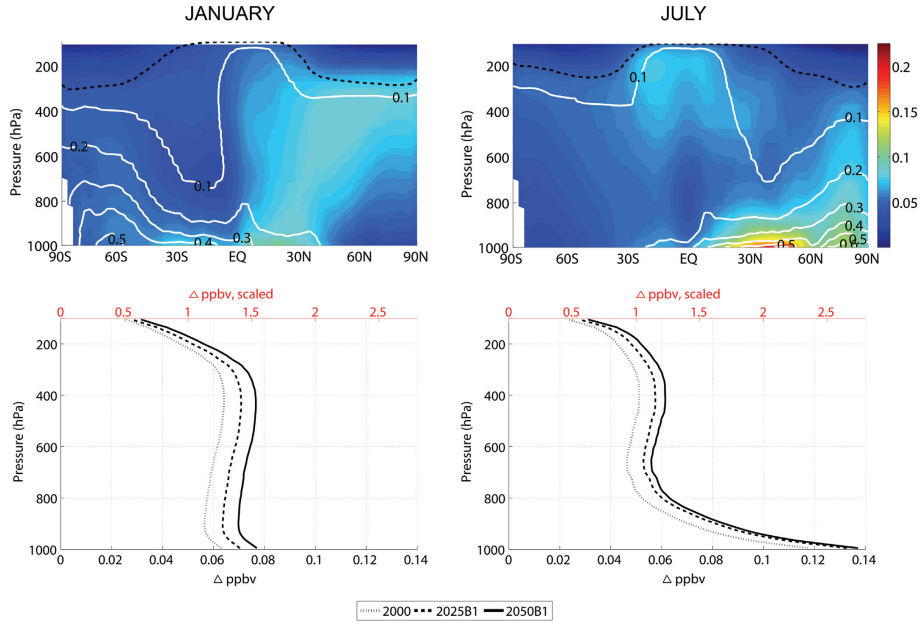

Fig. 8. Zonal mean perturbations of ozone (Δppbv) during January (left) and July (right) for the 2050 B1 scenario (top) and as Northern Hemisphere average for all years (bottom). In the top figures, solid contour lines show the change relative to the BASE simulation while the dashed line indicates the tropopause. The figures show the impact caused by a 5 % perturbation of ship emissions (simulations BASE–SHIP).

ACPD
11, 16801–16859, 2011

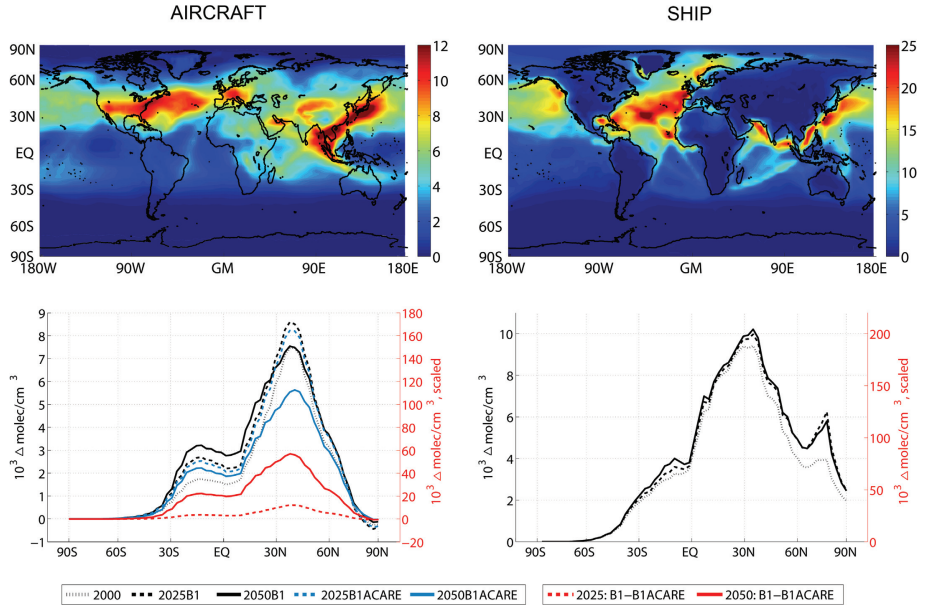

Fig. 9. Mean perturbations of OH (10^3 Δmolecules cm^{-3}) in July in the upper troposphere (300–200 hPa) due to a 5 % perturbation of aircraft emissions (left), and in the lower troposphere (> 800 hPa) due to a 5 % perturbation of ship emissions (right). The top row figures show results from the 2050 B1 scenario, and the bottom row figures show zonal means for all years and scenarios. The colorbars and the left *y*-axis show the unscaled impact of the 5 % perturbation of the emissions, while the red scales in the bottom figures are scaled up by a factor 20 from 5 % to 100 %. Note that different scales are used.

ACPD
11, 16801–16859, 2011

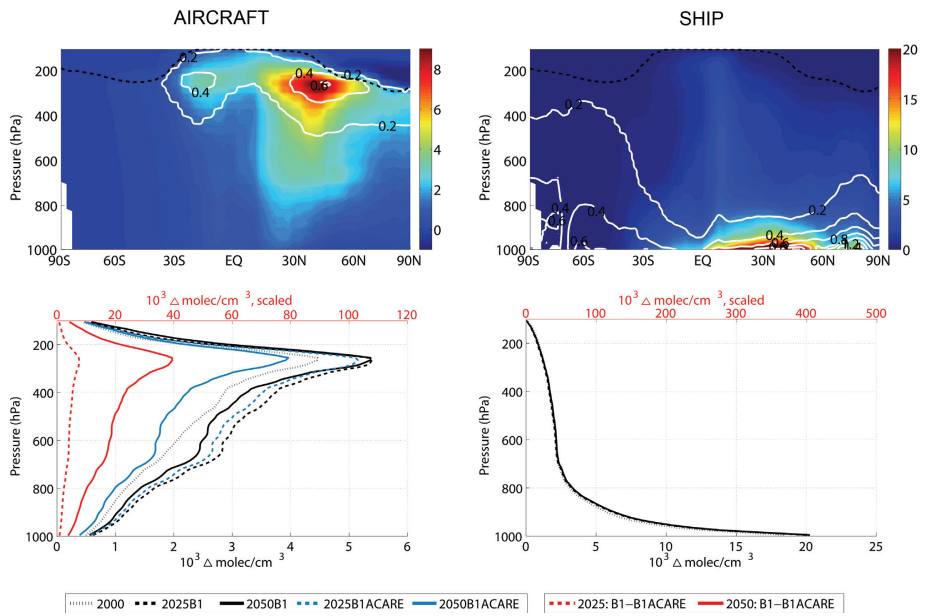

Fig. 10. Zonal mean perturbations of OH (10^3 Δmolecules cm^{-3}) in July due to a 5 % perturbation of aircraft emissions (left) and ship emissions (right), for the 2050 B1 scenario (top) and the average Northern Hemisphere vertical profile for all years and scenarios (bottom). In the top figures, solid contour lines show the change relative to the BASE simulation while the dashed line indicates the tropopause. The colorbar and the bottom *x*-axis show the unscaled impact of the 5 % perturbation of the emissions, while the red scales in the bottom figures are scaled up by a factor 20 from 5 % to 100 %. Note that different scales are used for AIR and SHIP.

ACPD
11, 16801–16859, 2011

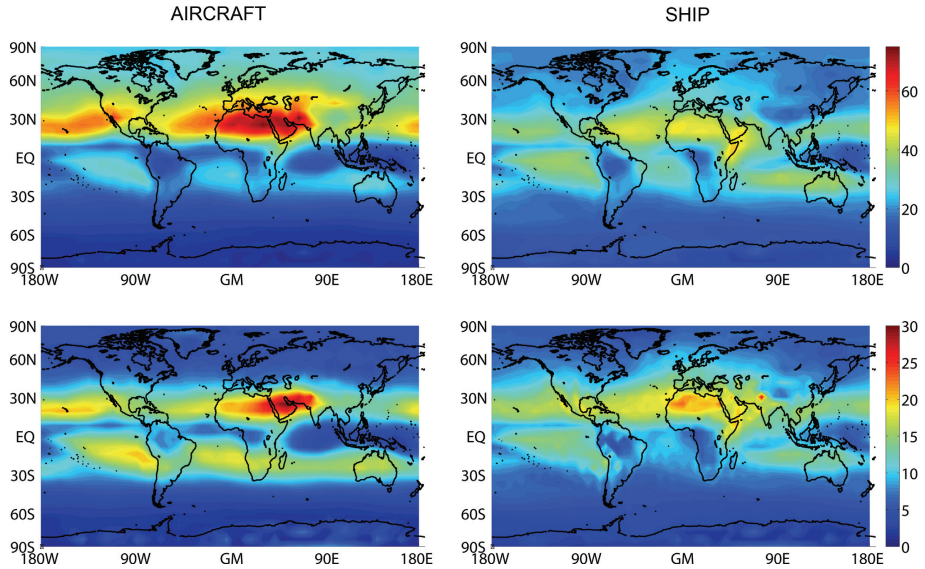

Fig. 11. Radiative forcing (mW m^{-2}) from short-term O_3 due to emissions from aircraft (left) and shipping (right), shown as ensemble mean for the 2050 B1 scenario (top) along with the absolute standard deviation (bottom). Note that the fully scaled perturbations were used to calculate the forcings.

ACPD
11, 16801–16859, 2011

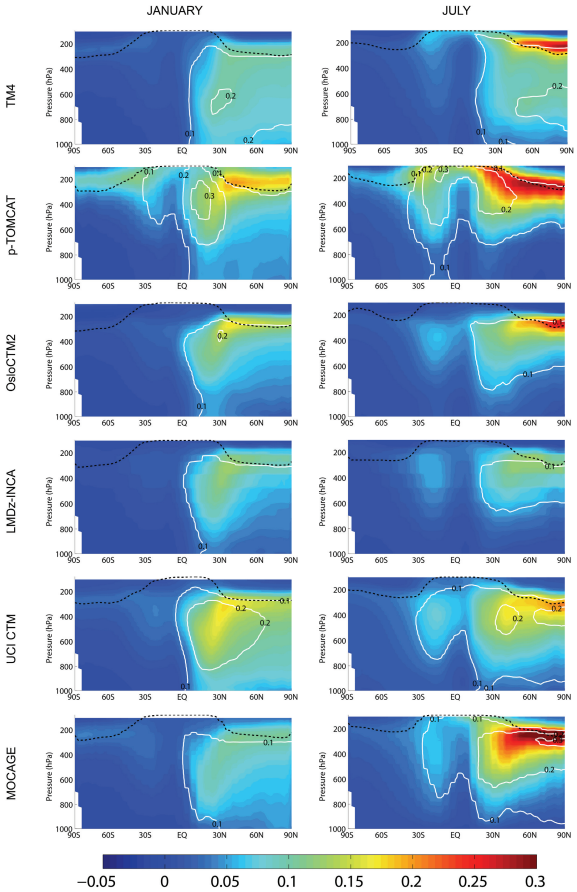

Fig. A1. Zonal mean perturbations of ozone (Δppbv) during January (left) and July (right) for the 2050 B1 scenario, due to a 5 % perturbation of aircraft emissions (simulations BASE–AIR). Solid contour lines show the change relative to the BASE simulation while the dashed line indicates the tropopause.

ACPD
11, 16801–16859, 2011

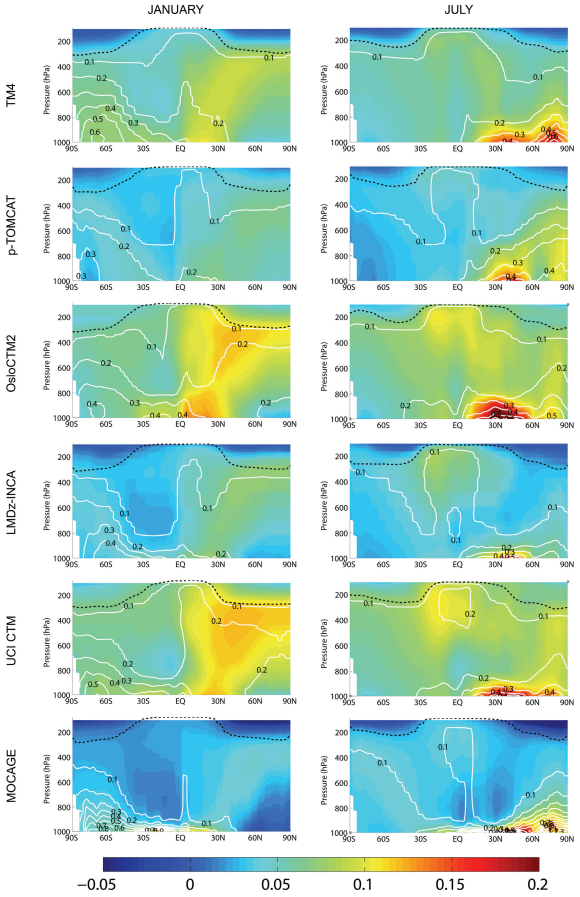

Fig. A2. Same as Fig. A1, but due to a 5 % perturbation of ship emissions (BASE–SHIP).

ACPD
11, 16801–16859, 2011